

## Inclusive quasielastic scattering of polarized electrons from polarized nuclei\*

J.E. Amaro<sup>1,2</sup>, J.A. Caballero<sup>3,4</sup>, T.W. Donnelly<sup>1</sup> and E. Moya de Guerra<sup>3</sup>

<sup>1</sup> Center for Theoretical Physics, Laboratory for Nuclear Science and Dept. of Physics, Massachusetts Institute of Technology, Cambridge, MA 02139, U.S.A.

<sup>2</sup> Departamento de Física Moderna, Universidad de Granada, Granada 18071, Spain

<sup>3</sup> Instituto de Estructura de la Materia, Consejo superior de Investigaciones Científicas, Serrano 123, Madrid 28006, Spain

<sup>4</sup> Departamento de Física Atómica, Molecular y Nuclear, Universidad de Sevilla, Apto 1065, Sevilla 41080, Spain.

### Abstract

The inclusive quasielastic response functions that appear in the scattering of polarized electrons from polarized nuclei are computed and analyzed for several closed-shell-minus-one nuclei with special attention paid to <sup>39</sup>K. Results are presented using two models for the ejected nucleon — when described by a distorted wave in the continuum shell model or by a plane wave in PWIA with on- and off-shell nucleons. Relativistic effects in kinematics and in the electromagnetic current have been incorporated throughout. Specifically, the recently obtained expansion of the electromagnetic current in powers only of the struck nucleon's momentum is employed for the on-shell current and the effects of the first-order terms (spin-orbit and convection) are compared with the zeroth-order (charge and magnetization) contributions. The use of polarized inclusive quasielastic electron scattering as a tool for determining near-valence nucleon momentum distributions is discussed.

\* This work is supported in part by funds provided by the U.S. Department of Energy (D.O.E.) under cooperative agreement #DE-FC01-94ER40818 (T.W.D. and J.E.A.), in part by DGICYT (Spain) under Contract Nos. PB92/0021-C02-01 and PB92-0927 and the Junta de Andalucía (Spain) and in part by NATO Collaborative Research Grant #940183.

MIT/CTP#2549

July 1996

# 1 Introduction

Inclusive quasielastic electron scattering is well-known as a way to probe the charge and current densities of individual nucleons within the nucleus. In this regime, at high momentum transfers  $q$  and for energy transfers  $\omega \cong \sqrt{q^2 + M^2} - M$ , where  $M =$  nucleon mass, single-nucleon knockout is expected to be dominant. The inclusive unpolarized reaction  $A(e, e')$  can be analyzed relatively directly in terms of the hadronic responses labeled  $L$  and  $T$  for longitudinal (charge) and transverse (current) contributions, respectively. To date the main attention has been on the completely unpolarized reaction, but now the study of electron scattering of polarized electrons from polarized nuclei is becoming feasible, due to recent technological advances in the development of polarized targets and high-duty-factor electron beams. The amount of nuclear structure information which is obtainable in such instances can be considerably richer than in the unpolarized case in that more responses of wider diversity can be studied [1]. While in other investigations devoted to polarization in quasielastic electron scattering the emphasis has been placed on the exclusive coincidence observables (see, for example, refs. [2], [3], [4] [5] and [6]), in this work our focus is on inclusive scattering with polarization degrees of freedom. Most such studies have been restricted to  ${}^2\vec{\text{H}}$  and  ${}^3\vec{\text{He}}$ , and include recent experimental asymmetry measurements [7, 8]; however, in this paper we restrict our attention entirely to polarization observables in (inclusive) quasielastic electron scattering from medium and heavy nuclei.

The organization of the paper is the following: in sect. 2 we present the formalism, centering the discussion around several issues. (1) We briefly review the essential expressions for the general nuclear polarized electromagnetic response functions based on the material presented in ref. [1] and establish the notation that follows. (2) We apply the above formalism to the particular case of one-hole nuclei in the continuum shell model (CSM) (see ref. [9]), with some details concerning the analytical sum over the angular momenta of the final hadronic state discussed in appendix

A and concerning the Coulomb multipoles for the spin-orbit charge density placed in appendix B. While for the sake of brevity our focus is placed on one-proton-hole cases, the approach is straightforwardly applied to one-neutron-hole nuclei as well as to nuclei having a single nucleon above a closed shell. In the present work when using the CSM we take the mean field in initial and final states to be the same, thereby maintaining the orthogonality of the single-particle wave functions. Clearly at high outgoing nucleon energies this exaggerates the final-state interactions (FSI) and thus we contrast this approach with the Plane Wave Impulse Approximation (PWIA). Accordingly, (3) we summarize the essence of the PWIA for both on- and off-shell single-nucleon currents. Indeed, one of our motivations in the present work is to explore the evolution from the low-energy regime where final-state interactions (FSI) are important to higher energies where they are not and where the PWIA is expected to be valid. Intercomparisons of the CSM and PWIA results will also serve in explaining many of the features of the spin observables. In discussing the PWIA we obtain the polarized responses for the case of a one-hole nucleus (again, with some details of the calculation presented in appendix C) and introduce a version of the model where the (usually off-shell) relativistic single-nucleon current is replaced by the on-shell form used in recent work with promising results [10]. This current involves an expansion only in powers of  $\eta \equiv p/M$ , with  $p$  the bound nucleon momentum, and importantly not in  $\kappa \equiv q/2M$  or  $\lambda \equiv \omega/2M$ .

In sect. 3 we present the results for the response functions of a few selected one-proton-hole nuclei. The discussions in this section start with a re-examination of the elastic scattering of polarized electrons from a polarized proton at rest, where we know the exact answer, in order to provide some insight into the cases of polarized protons in  $1s_{1/2}$ ,  $1p_{1/2}$  and  $2s_{1/2}$  shells. The results in these cases are contrasted with those for  $1p_{3/2}$  and  $1d_{3/2}$  polarized protons, the last being the case that is then studied in more detail, namely, the nucleus  $^{39}\text{K}$ . In the course of presenting our results we study the effects due to distortion in the ejected nucleon wave function caused by the real nuclear mean field, as well as the effects of the first-order ( $\eta$ -dependent)

terms in the nuclear current; second-order terms are also briefly discussed here. On- and off-shell versions of the PWIA are compared with each other and with the  $\eta$ -dependent effects. We discuss the sensitivity of the polarized responses to the actual orbit containing the polarized nucleon and how this has the potential to be a powerful new tool for determining the near-valence-shell nucleon momentum distribution. Finally, in sect. 4, we draw our conclusions.

## 2 Formalism

### 2.1 Polarized cross section

We consider a nucleus  $A$  in an initial state polarized in direction  $\Omega^* = (\theta^*, \phi^*)$ , denoted  $|A\rangle = |i(\Omega^*)\rangle$ , from which a polarized electron with helicity  $h$  is scattered, leaving the nucleus in a final state  $|f\rangle$  lying in the continuum. In the approximation that the electron is described by plane waves, the inclusive cross section in the laboratory system may be written in terms of six nuclear response functions [1]:

$$\frac{d^2\sigma}{d\epsilon'_e d\Omega'_e} = \sigma_M \left[ \sum_K v_K R^K + h \sum_{K'} v_{K'} R^{K'} \right], \quad (1)$$

where  $Q^\mu = (\omega, \mathbf{q})$  is the four-momentum transfer,  $\epsilon'_e$  and  $\Omega'_e$  are the energy and angles of the final electron,  $\sigma_M$  is the Mott cross section and the summation indices are  $K = L, T, TL, TT$  and  $K' = T', TL'$ . If the extreme relativistic limit is assumed for the electron and we refer to a coordinate system with the  $z$ -axis along  $\mathbf{q}$  and the  $x$ -axis in the scattering plane, the kinematic factors  $v_K$  and  $v_{K'}$  can be written as

$$v_L = \left( \frac{Q^2}{q^2} \right)^2, \quad v_T = \tan^2 \frac{\theta_e}{2} - \frac{Q^2}{2q^2}, \quad (2)$$

$$v_{TL} = \frac{1}{\sqrt{2}} \frac{Q^2}{q^2} \sqrt{\tan^2 \frac{\theta_e}{2} - \frac{Q^2}{q^2}}, \quad v_{TT} = \frac{Q^2}{2q^2}, \quad (3)$$

$$v_{T'} = \tan \frac{\theta_e}{2} \sqrt{\tan^2 \frac{\theta_e}{2} - \frac{Q^2}{q^2}}, \quad v_{TL'} = \frac{1}{\sqrt{2}} \frac{Q^2}{q^2} \tan \frac{\theta_e}{2}. \quad (4)$$

Here we use  $Q_\mu Q^\mu \equiv Q^2 = \omega^2 - q^2 < 0$  and  $\theta_e$  is the electron scattering angle. The inclusive nuclear responses  $R^K, R^{K'}$  are the components

$$R^L = W^{00}, \quad R^T = W^{xx} + W^{yy} \quad (5)$$

$$R^{TL} = \sqrt{2}(W^{0x} + W^{x0}), \quad R^{TT} = W^{yy} - W^{xx} \quad (6)$$

$$R^{T'} = i(W^{xy} - W^{yx}), \quad R^{TL'} = i\sqrt{2}(W^{0y} - W^{y0}) \quad (7)$$

of the nuclear electromagnetic tensor defined by

$$W^{\mu\nu} = \sum_f \delta(E_f - E_i - \omega) \langle f | \hat{J}^\mu(\mathbf{q}) | i \rangle^* \langle f | \hat{J}^\nu(\mathbf{q}) | i \rangle. \quad (8)$$

Here the sum runs over all the final nuclear states  $|f\rangle$  with energy  $E_f = E_i + \omega$  and

$$\hat{J}^\mu(\mathbf{q}) = \int d^3r e^{i\mathbf{q}\cdot\mathbf{r}} \hat{j}^\mu(\mathbf{r}) \quad (9)$$

is the Fourier transform of the nuclear electromagnetic operator.

## 2.2 Multipole analysis of the polarized responses

We now consider the case when the initial nuclear state of spin  $J_i$  is fully polarized in the direction  $\Omega^* = (\theta^*, \phi^*)$ , where the spherical coordinates for the polarization axis are taken with respect the coordinate system described above (see the developments in refs. [1] and [2] for details). Using rotation matrices the initial nuclear wave function can be expressed in terms of states  $|J_i M_i\rangle$  for which the axis of quantization is  $\mathbf{q}$ :

$$|i\rangle = |J_i J_i(\Omega^*)\rangle = \sum_{M_i} \mathcal{D}_{M_i J_i}^{(J_i)}(\Omega^*) |J_i M_i\rangle. \quad (10)$$

We must sum over all the final nuclear states and thus we may also use a basis of final states with good angular momentum having  $\mathbf{q}$  as the axis of quantization,  $|f\rangle = |J_f M_f\rangle$ . The charge and transverse current operators may be developed as sums of multipoles in the usual way:

$$\hat{\rho}(\mathbf{q}) = \sqrt{4\pi} \sum_J i^J [J] \hat{M}_{J0}(q) \quad (11)$$

$$\hat{J}_M(\mathbf{q}) = -\sqrt{2\pi} \sum_J i^J [J] \left[ \hat{T}_{JM}^{el}(q) + M \hat{T}_{JM}^{mag}(q) \right], \quad (12)$$

where  $M$  is the index of the spherical components and  $\hat{M}_{JM}$ ,  $\hat{T}_{JM}^{el}$  and  $\hat{T}_{JM}^{mag}$  are the usual Coulomb (CJ), electric (EJ) and magnetic (MJ) multipoles. Throughout we use the notation  $[J] \equiv \sqrt{2J+1}$  for any angular momentum variable  $J$ .

Using the above expansion, the nuclear tensor can be written as a sum of factors of the kind

$$B_{J'J}^{M'M} = \sum_{M_f M_i M'_i} \mathcal{D}_{M_i J_i}^{(J_i)*} \mathcal{D}_{M'_i J_i}^{(J_i)} \langle J_f M_f | \hat{T}'_{J' M'} | J_i M_i \rangle^* \langle J_f M_f | \hat{T}_{JM} | J_i M'_i \rangle, \quad (13)$$

where  $T$  and  $T'$  are any of the  $C$ ,  $E$  or  $M$  operators. The dependence on the polarization axis in the product of two rotation matrices can be developed in spherical harmonics

$$\mathcal{D}_{M_i J_i}^{(J_i)*} \mathcal{D}_{M'_i J_i}^{(J_i)} = \sqrt{4\pi} \sum_{\mathcal{J} \mathcal{M}} (-1)^{J_i + M_i + \mathcal{J}} \begin{pmatrix} J_i & J_i & \mathcal{J} \\ -M_i & M'_i & \mathcal{M} \end{pmatrix} f_{\mathcal{J}}^i Y_{\mathcal{J} \mathcal{M}}(\Omega^*), \quad (14)$$

where  $f_{\mathcal{J}}^i$  is the Fano tensor for 100% polarization,  $f_{\mathcal{J}}^i = \langle J_i J_i J_i - J_i | \mathcal{J} 0 \rangle$ . Then using the Wigner-Eckart theorem and summing over third components, one obtains the following dependence involving the polarization angles and the reduced matrix elements of the different multipole operators (see ref. [1] for details):

$$B_{J'J}^{M'M} = \sum_{\mathcal{J} \mathcal{M}} (-1)^{J_i + J_f + M + \mathcal{M}} [\mathcal{J}] \left[ \frac{(\mathcal{J} - \mathcal{M})!}{(\mathcal{J} + \mathcal{M})!} \right]^{1/2} \begin{pmatrix} J' & J & \mathcal{J} \\ M' & -M & \mathcal{M} \end{pmatrix} \\ \times \begin{Bmatrix} J' & J & \mathcal{J} \\ J_i & J_i & J_f \end{Bmatrix} f_{\mathcal{J}}^i P_{\mathcal{J}}^{\mathcal{M}}(\cos \theta^*) e^{i\mathcal{M}\phi^*} \langle J_f || \hat{T}'_{J'} || J_i \rangle^* \langle J_f || \hat{T}_J || J_i \rangle, \quad (15)$$

where  $P_{\mathcal{J}}^{\mathcal{M}}(\cos \theta^*)$  is an associated Legendre function (we use the conventions of ref. [11]).

Now taking the appropriate components of the nuclear tensor and defining the (real) Coulomb, electric and magnetic multipoles

$$T_{CJ} \equiv \langle J_f || \hat{M}_J(q) || J_i \rangle \quad (16)$$

$$T_{EJ} \equiv \langle J_f || \hat{T}_J^{el}(q) || J_i \rangle \quad (17)$$

$$T_{MJ} \equiv \langle J_f || i \hat{T}_J^{mag}(q) || J_i \rangle, \quad (18)$$

we arrive at the following equations for the polarized quasielastic responses [1]:

$$R^L = 4\pi \sum_{\mathcal{J}} P_{\mathcal{J}}^+ P_{\mathcal{J}}(\cos \theta^*) f_{\mathcal{J}}^i W_{\mathcal{J}}^L(q, \omega) \quad (19)$$

$$R^T = 4\pi \sum_{\mathcal{J}} P_{\mathcal{J}}^+ P_{\mathcal{J}}(\cos \theta^*) f_{\mathcal{J}}^i W_{\mathcal{J}}^T(q, \omega) \quad (20)$$

$$R^{TL} = 4\pi \sum_{\mathcal{J} \geq 2} P_{\mathcal{J}}^+ P_{\mathcal{J}}^1(\cos \theta^*) \cos \phi^* f_{\mathcal{J}}^i W_{\mathcal{J}}^{TL}(q, \omega) \quad (21)$$

$$R^{TT} = 4\pi \sum_{\mathcal{J} \geq 2} P_{\mathcal{J}}^+ P_{\mathcal{J}}^2(\cos \theta^*) \cos 2\phi^* f_{\mathcal{J}}^i W_{\mathcal{J}}^{TT}(q, \omega) \quad (22)$$

$$R^{T'} = 4\pi \sum_{\mathcal{J}} P_{\mathcal{J}}^- P_{\mathcal{J}}(\cos \theta^*) f_{\mathcal{J}}^i W_{\mathcal{J}}^{T'}(q, \omega) \quad (23)$$

$$R^{TL'} = 4\pi \sum_{\mathcal{J}} P_{\mathcal{J}}^- P_{\mathcal{J}}^1(\cos \theta^*) \cos \phi^* f_{\mathcal{J}}^i W_{\mathcal{J}}^{TL'}(q, \omega), \quad (24)$$

where the parity projectors  $P_{\mathcal{J}}^{\pm} \equiv [1 + (-1)^{\mathcal{J}}]/2$  have been used. The above expressions show that several sets of measurements with different polarization angles  $\Omega^*$  in principle lead to the separation of the reduced nuclear responses  $W_{\mathcal{J}}^K(q, \omega)$ ; these are functions only of the energy and momentum transfer and are given by the following: for  $\mathcal{J} = \text{even}$

$$W_{\mathcal{J}}^L = \sum_f \delta(E_f - E_i - \omega) \sum_{J'J} \Lambda_{fi}(J', J, \mathcal{J}, 0, 0, 0) \xi_{J'J}^+ T_{CJ'} T_{CJ} \quad (25)$$

$$W_{\mathcal{J}}^T = -\sum_f \delta(E_f - E_i - \omega) \sum_{J'J} \Lambda_{fi}(J', J, \mathcal{J}, 1, -1, 0) \\ \times [\xi_{J'J}^+(T_{EJ'} T_{EJ} + T_{MJ'} T_{MJ}) + \xi_{J'J}^-(T_{EJ'} T_{MJ} - T_{MJ'} T_{EJ})] \quad (26)$$

$$W_{\mathcal{J}}^{TL} = 2\sqrt{2} \sum_f \delta(E_f - E_i - \omega) \sum_{J'J} \Lambda_{fi}(J', J, \mathcal{J}, 0, 1, -1) \\ \times T_{CJ'} (\xi_{J'J}^+ T_{EJ} - \xi_{J'J}^- T_{MJ}) \quad (27)$$

$$W_{\mathcal{J}}^{TT} = -\sum_f \delta(E_f - E_i - \omega) \sum_{J'J} \Lambda_{fi}(J', J, \mathcal{J}, 1, 1, -2) \\ \times [\xi_{J'J}^+(T_{EJ'} T_{EJ} - T_{MJ'} T_{MJ}) - \xi_{J'J}^-(T_{EJ'} T_{MJ} + T_{MJ'} T_{EJ})], \quad (28)$$

whereas for  $\mathcal{J} = \text{odd}$ ,  $W_{\mathcal{J}}^T \rightarrow W_{\mathcal{J}}^{T'}$  and  $W_{\mathcal{J}}^{TL} \rightarrow -W_{\mathcal{J}}^{TL'}$  (see ref. [1]). We use the notation

$$\Lambda_{fi}(J', J, \mathcal{J}, M', M, \mathcal{M}) \equiv [J][J'][\mathcal{J}] (-1)^{J_i + J_f} \left[ \frac{(\mathcal{J} - |\mathcal{M}|)!}{(\mathcal{J} + |\mathcal{M}|)!} \right]^{1/2} \\ \times \begin{pmatrix} J' & J & \mathcal{J} \\ M' & M & \mathcal{M} \end{pmatrix} \left\{ \begin{matrix} J' & J & \mathcal{J} \\ J_i & J_i & J_f \end{matrix} \right\} \quad (29)$$



and

$$\xi_{J'J}^+ \equiv (-1)^{(J'-J)/2} P_{J'+J}^+, \quad \xi_{J'J}^- \equiv (-1)^{(J'-J+1)/2} P_{J'+J}^-. \quad (30)$$

These equations are general for any nucleus. In the next section we apply them to the particular case of a one-hole nucleus.

### 2.3 Polarized responses for a one-hole nucleus

In this work we consider closed-shell-minus-one nuclei where the initial nuclear state is obtained as a hole in a closed-shell core  $|C\rangle$ :

$$|A\rangle = |i^{-1}(\Omega^*)\rangle = \sum_{m_i} \mathcal{D}_{m_i j_i}^{(j_i)}(\Omega^*) b_{i, m_i}^\dagger |C\rangle, \quad (31)$$

where  $|i\rangle = |n_i, l_i, j_i\rangle$  is a single-particle state occupied in the core and  $b_{i, m_i}^\dagger$  is the creation operator for a hole,  $b_{i, m_i}^\dagger = (-1)^{j_i+m_i} a_{i, -m_i}$ . Here we follow the convention of using lower case letters  $j_i$  for half-integer angular momenta. As in the present work we only consider the one-body piece of the electromagnetic nuclear current, the interaction with the virtual photon gives rise only to particle-hole (p-h) excitations. Thus the final nuclear states are described by

$$|f\rangle = |p, (h^{-1}, i^{-1})J_B; j_f\rangle. \quad (32)$$

Here  $|h\rangle = |n_h, l_h, j_h\rangle$  is another (bound) single-particle state in the core, while  $|p\rangle = |\epsilon_p, l_p, j_p\rangle$  is a particle in the continuum. The residual nucleus is a two-hole nucleus  $|B\rangle = |(h^{-1}, i^{-1})J_B\rangle$  with total angular momentum  $J_B$ , and it is coupled with the outgoing particle  $|p\rangle$  to a total angular momentum  $j_f$ . In the present work the wave functions of the single-particle states are obtained using a mean-field potential of Woods-Saxon type, for both negative (bound) and positive (continuum) energies. More details on this aspect of the calculation, including the values of the potential parameters, can be found in refs. [9] and [10].

The sum over final states to obtain the inclusive responses now runs over all the holes  $h$ , particles  $p$ , and angular momenta  $J_B$  and  $j_f$ . In appendix A we show how

the sums over  $J_B$  and  $j_f$  can be performed using Racah algebra. The final reduced responses can be written in terms of the single-particle reduced matrix elements taken between particle and hole states

$$t_{CJ} \equiv \langle p || M_J(q) || h \rangle \quad (33)$$

$$t_{EJ} \equiv \langle p || T_J^{el}(q) || h \rangle \quad (34)$$

$$t_{MJ} \equiv \langle p || iT_J^{mag}(q) || h \rangle, \quad (35)$$

using lower-case letters to distinguish the particle-hole multipole matrix elements from their many-body counterparts in eqs. (16–18), and yield the following expressions for the reduced responses:

$$\begin{aligned} W_{\mathcal{J}}^L &= \delta_{\mathcal{J}0}[j_i] \sum_{ph} \delta(\epsilon_p - \epsilon_h - \omega) \sum_J t_{CJ}^2 \\ &\quad - \sum_{ph} \delta_{hi} \delta(\epsilon_p - \epsilon_h - \omega) \sum_{J'J} \Lambda_{ph}(J', J, \mathcal{J}, 0, 0, 0) \xi_{J'J}^+ t_{CJ'} t_{CJ} \end{aligned} \quad (36)$$

$$\begin{aligned} W_{\mathcal{J}}^T &= \delta_{\mathcal{J}0}[j_i] \sum_{ph} \delta(\epsilon_p - \epsilon_h - \omega) \sum_J (t_{EJ}^2 + t_{MJ}^2) \\ &\quad + (-1)^{\mathcal{J}} \sum_{ph} \delta_{pi} \delta(\epsilon_p - \epsilon_h - \omega) \sum_{J'J} \Lambda_{ph}(J', J, \mathcal{J}, 1, -1, 0) \\ &\quad \times [\xi_{J'J}^+ (t_{EJ'} t_{EJ} + t_{MJ'} t_{MJ}) + \xi_{J'J}^- (t_{EJ'} t_{MJ} - t_{MJ'} t_{EJ})] \end{aligned} \quad (37)$$

$$\begin{aligned} W_{\mathcal{J}}^{TL} &= -2\sqrt{2}(-1)^{\mathcal{J}} \sum_{ph} \delta_{hi} \delta(\epsilon_p - \epsilon_h - \omega) \sum_{J'J} \Lambda_{ph}(J', J, \mathcal{J}, 0, 1, -1) \\ &\quad \times t_{CJ'} (\xi_{J'J}^+ t_{EJ} - \xi_{J'J}^- t_{MJ}) \end{aligned} \quad (38)$$

$$\begin{aligned} W_{\mathcal{J}}^{TT} &= (-1)^{\mathcal{J}} \sum_{ph} \delta_{pi} \delta(\epsilon_p - \epsilon_h - \omega) \sum_{J'J} \Lambda_{ph}(J', J, \mathcal{J}, 1, 1, -2) \\ &\quad \times [\xi_{J'J}^+ (t_{EJ'} t_{EJ} - t_{MJ'} t_{MJ}) - \xi_{J'J}^- (t_{EJ'} t_{MJ} + t_{MJ'} t_{EJ})] \end{aligned} \quad (39)$$

$$\begin{aligned} W_{\mathcal{J}}^{T'} &= (-1)^{\mathcal{J}} \sum_{ph} \delta_{pi} \delta(\epsilon_p - \epsilon_h - \omega) \sum_{J'J} \Lambda_{ph}(J', J, \mathcal{J}, 1, -1, 0) \\ &\quad \times [\xi_{J'J}^+ (t_{EJ'} t_{EJ} + t_{MJ'} t_{MJ}) + \xi_{J'J}^- (t_{EJ'} t_{MJ} - t_{MJ'} t_{EJ})] \end{aligned} \quad (40)$$

$$W_{\mathcal{J}}^{TL'} = -W_{\mathcal{J}}^{TL}. \quad (41)$$

Note that although formally  $W_{\mathcal{J}}^{TL'} = -W_{\mathcal{J}}^{TL}$ , in practice they are quite different because of the different  $\mathcal{J}$ -values (the same comment applies to  $W_{\mathcal{J}}^{T'}$  versus  $W_{\mathcal{J}}^T$ ). We shall see in the next section that an explicit calculation in PWIA shows that actually the primed and unprimed responses have quite different analytical forms.

Some comments about the above equations are now in order.

1. The polarized responses for the case of one particle above a closed shell are simply related to these one-hole results:

$$\left(W_{\mathcal{J}}^K\right)_{\text{particle}} = -(-1)^{\mathcal{J}} \left(W_{\mathcal{J}}^K\right)_{\text{hole}}. \quad (42)$$

2. The first terms in the  $L$  and  $T$  responses only contribute for  $\mathcal{J} = 0$  and they give rise to the unpolarized responses of the closed-shell nucleus  $|C\rangle$ . In fact, for  $\mathcal{J} = 0$  we have the Fano tensor  $f_0^i = 1/[j_i]$  and the Legendre function  $P_0(\cos \theta^*) = 1$ , leading to the following piece in the longitudinal response

$$\begin{aligned} 4\pi \sum_{\mathcal{J}} P_{\mathcal{J}}(\cos \theta^*) f_{\mathcal{J}}^i \delta_{\mathcal{J}0} [j_i] \sum_{phJ} \delta(\epsilon_p - \epsilon_h - \omega) t_{CJ}^2 \\ = 4\pi \sum_{phJ} \delta(\epsilon_p - \epsilon_h - \omega) t_{CJ}^2 \end{aligned} \quad (43)$$

and a similar term for the transverse response.

3. The second term of  $W_{\mathcal{J}}^L$  or  $W_{\mathcal{J}}^T$  only contributes for  $h = i$  and corresponds to the response of the hole; it must be subtracted from the total response of the core to obtain the total response of the nucleus. For example, for  $\mathcal{J} = 0$  we have  $\Lambda_{pi}(J, J, 0, 0, 0, 0) = 1/[j_i]$  and thus obtain for the  $W_0^L$ -response

$$W_0^L = \sum_{phJ} \delta(\epsilon_p - \epsilon_h - \omega) [j_i] \left(1 - \frac{\delta_{hi}}{2j_i + 1}\right) t_{CJ}^2, \quad (44)$$

that is, the total unpolarized response of the core minus the response of the hole.

4. For the polarized responses TL, TT, T' and TL' only the shell containing the hole contributes. Note that when one has a single particle outside a closed-shell core then these contributions behave as shown in eq. (42).
5. For the electromagnetic current operators we use the non-relativistic reduction whose expressions are given below (eqs. (50), (71-73)). The time component

is the sum of charge plus spin-orbit operators, while the spatial component is the sum of magnetization plus convection operators. The reduced matrix elements of the (charge) Coulomb, and (magnetization and convection) electric and magnetic operators are given in ref. [10]. Note that, although we have maintained the traditional names for these terms, actually they differ slightly from the traditional charge, magnetization and convection operators. In the present work we include the spin-orbit operator which is usually not included in non-relativistic electron scattering calculations, since it is assumed to be small. As we shall see, the spin-orbit contributions do turn out to be small for the unpolarized responses, but are important for some of the polarized ones (especially the TL response) at the values of the momentum transfer used in this work. The reduced matrix elements of the Coulomb operator for the spin-orbit term are computed in appendix B.

6. In all the calculations that follow we employ relativistic kinematics. This means that from the (non-relativistic) energy of the emitted nucleon  $\epsilon_p = \epsilon_h + \omega$  we compute the momentum  $\mathbf{p}'$  of the particle in PWIA from the relativistic energy-momentum relation

$$\begin{aligned} p'^2 &= (M + \epsilon_p)^2 - M^2 = \epsilon_p(\epsilon_p + 2M) \\ &= 2M \left[ \omega \left( 1 + \frac{\omega}{2M} \right) + \epsilon_h + \epsilon_h \frac{2\omega + \epsilon_h}{2M} \right]. \end{aligned} \quad (45)$$

When the final-state interactions are present (*i.e.*, in the CSM) we solve the equivalent Schrödinger equation with eigenvalue  $\epsilon_p(1 + \epsilon_p/2M)$ . Note that this procedure is equivalent to solving a Klein-Gordon equation  $(-\nabla^2 + M^2 + 2MV)\psi = E_p^2\psi$ , with  $V$  the Woods-Saxon potential and  $E_p = \epsilon_p + M$  the relativistic energy of the particle. An alternative, convenient prescription to implement the above relativistic kinematics was employed in ref. [10] (see also ref. [12]), that of making the replacement  $\omega \rightarrow \omega(1 + \omega/2M)$  in the non-relativistic nuclear responses, but not in the single-nucleon form factors (where the asymptotic momentum is computed as  $p'^2 = 2M(\omega + \epsilon_h)$ ).

Clearly this is equivalent to the above equation (45) provided that the last term  $\epsilon_h(2\omega + \epsilon_h)/2M$  can be neglected, which is a good approximation at the energies considered in this work.

7. The sums over multipoles  $J, J'$  are infinite and, in practice, we must sum all multipoles until convergence is reached. The number of multipoles needed grows with the mass number  $A$  and with the momentum transfer, as detailed in table 2 of ref. [10]. Indeed, in this work we were able to test the degree of convergence by examining the particular case where  $V = 0$  for the final state (but not for the initial) using two different approaches, with the multipole expansion and with the factorization procedure in PWIA — the results obtained were indistinguishable.

## 2.4 Polarized responses in PWIA

The multipole expansions introduced in the last section may therefore also be applied when we make the approximation in which the particle  $p$  is a free (non-interacting) wave function and so described as a plane wave function or, in a multipole analysis, a spherical Bessel function. Additional reasons for considering the plane-wave outgoing nucleon approximation, beyond being a test of convergence, are the following. First, we want to analyze the effects arising from the distortion of the ejected particle due to the mean field in the final state and compare these with the results obtained with a pure plane wave. Note that in our treatment the distortion is caused by a *real* mean-field potential. Therefore there is no absorption due to inelastic processes in the exit channel. The reduction of flux can be treated at least approximately *a posteriori* by using a phenomenological model of final-state interaction that takes care of those effects through the introduction of a self-energy for the particle-hole propagator. Alternatively, these effects could also be simulated by a phenomenological optical potential in the exit channel, although this raises the issue of lack of orthogonality in the wave functions. The study of such additional FSI effects in the

polarized responses is left for a forthcoming paper and here we only deal with pure distortion effects caused by the nuclear mean field.

Second, for the values of the momentum transfer ( $q \sim 500$  MeV/c) that we are considering here the energy of the outgoing nucleon in the quasielastic region is very high in comparison with the energy of the bound nucleons. This is especially true in the case of the polarization-dependent responses, where only the outer shell contributes. Thus the approximation of plane waves for the ejected nucleon should give reasonable results. The advantage of the PWIA approach is that we can perform part of the calculation analytically and can factorize the responses into a product of two terms, the first containing the single-nucleon responses and the second the spectral function of the polarized nucleus. This later approximation is very useful when attempting to disentangle contributions from different terms in the nuclear current operator (spin-orbit, convection, higher-order momentum-dependent terms, ...).

#### 2.4.1 Factorization of the responses

We begin with the exclusive process  $\vec{A}(\vec{e}, e'N)B$  in which the ejected nucleon has momentum  $\mathbf{p}'$  and the residual nucleus is left in the state  $|B\rangle$ . The exclusive cross section for such a process is given by (*cf.* eq. (1))

$$\frac{d^3\sigma}{d\epsilon'_e d\Omega'_e d\Omega'} = \sigma_M \left[ \sum_K v_K \mathcal{R}_B^K + h \sum_{K'} v_{K'} \mathcal{R}_B^{K'} \right], \quad (46)$$

where  $\mathcal{R}_B^{K,K'}$  are the exclusive responses. The inclusive responses  $R^K$  are obtained by integration over the nucleon angles and summing over the states  $|B\rangle$  of the residual nuclear system

$$R^{K,K'} = \sum_B \int d\Omega' \mathcal{R}_B^{K,K'}(\Omega) = \sum_B R_B^{K,K'}. \quad (47)$$

The inclusive cross section is given again by eq. (1). The exclusive responses are combinations of the exclusive hadronic tensor in PWIA

$$W_B^{\mu\nu} = Mp' \sum_{s'M_B} \langle \mathbf{p}' s' B | J^\mu(\mathbf{q}) | A \rangle^* \langle \mathbf{p}' s' B | J^\nu(\mathbf{q}) | A \rangle, \quad (48)$$

where  $\langle \mathbf{p}'s'B \rangle$  corresponds to a final state having an on-shell plane-wave nucleon with momentum  $\mathbf{p}'$  and spin projection  $s'$ , together with the daughter nucleus in some state labeled  $B$ .

The details of proceeding in the usual approach to spin-dependent PWIA studies with off-shell single-nucleon currents  $CC1$ ,  $CC2$ , *etc.*, are given in refs. [5, 13, 14] and will not be repeated here. Instead, here we specialize the formalism to the situation where we take the PWIA with an on-shell current, specifically, the one developed in ref. [10]. In the next section results are presented for both on- and off-shell cases. Proceeding with the former, the coordinate-space plane-wave nucleon's wave function is given by

$$\langle \mathbf{r} | \mathbf{p}'s' \rangle = (2\pi)^{-3/2} e^{i\mathbf{p}' \cdot \mathbf{r}} \chi_{s'} \quad (49)$$

with energy  $E_{p'} = \omega + M_A - E_B = \sqrt{p'^2 + M^2}$ . Here only two-component spin spinors occur, since the lower-component information that is usually explicit in the PWIA has been incorporated in the current operators (see [10]). A sum is then performed over the spin  $s'$  and the orientation  $M_B$  of the residual nucleus, since in the present work it is assumed that the polarizations of the final particles are undetected. The factor  $Mp'$  in eq. (48) comes from the change of normalization in the outgoing nucleon wave function, *i.e.*, in the CSM the particle wave functions are normalized with a  $\delta$ -function containing energies, while the outgoing nucleon wave functions, eq. (49), are standard plane waves normalized with a  $\delta$ -function of momentum. The factorization of the hadronic tensor follows from the translational invariance of the nuclear electromagnetic current,

$$\langle \mathbf{p}'r' | J^\mu(\mathbf{q}) | \mathbf{p}r \rangle = \delta(\mathbf{p} + \mathbf{q} - \mathbf{p}') J^\mu(\mathbf{p}', \mathbf{p})_{r'r}, \quad (50)$$

thereby yielding the current spin-matrix  $J^\mu(\mathbf{p}', \mathbf{p})_{r'r}$  to be used below. The most general form of this matrix is

$$J^\mu = a^\mu + i\mathbf{b}^\mu \cdot \boldsymbol{\sigma}. \quad (51)$$

We must make the approximation that the ground state  $|A\rangle$  has no components with momentum  $\mathbf{p}'$ , that is,  $a_{\mathbf{p}'s'}|A\rangle \simeq 0$ . As a consequence, one can easily show that the hadronic tensor can be written as a trace of the product of two spin matrices

$$W_B^{\mu\nu} = M p' \text{Tr} [w^{\mu\nu}(\mathbf{p}', \mathbf{p}) n_B(\mathbf{p})], \quad (52)$$

where the missing momentum  $\mathbf{p} = \mathbf{p}' - \mathbf{q}$  has been introduced, the single-nucleon tensor is given by

$$w^{\mu\nu}(\mathbf{p}', \mathbf{p})_{rr'} = \sum_s J^\mu(\mathbf{p}', \mathbf{p})_{sr}^* J^\nu(\mathbf{p}', \mathbf{p})_{sr'}, \quad (53)$$

and  $n_B(\mathbf{p})$  is the partial momentum distribution matrix for residual nucleus  $|B\rangle$

$$n_B(\mathbf{p})_{r'r} = \sum_{M_B} \langle B | a_{\mathbf{p}r} | A \rangle^* \langle B | a_{\mathbf{p}r'} | A \rangle. \quad (54)$$

Note that the diagonal element  $n_B(\mathbf{p})_{rr}$  is the probability that the nucleus  $|A\rangle$  be a residual nucleus  $|B\rangle$  plus a particle with momentum  $\mathbf{p}$  and third spin component  $r$ . Note also that the responses defined in eqs. (5, 6) involve combinations of the form

$$w^K \sim J^{\mu\dagger} J^\nu + J^{\nu\dagger} J^\mu = 2(a^\mu a^\nu + \mathbf{b}^\mu \cdot \mathbf{b}^\nu), \quad (55)$$

for  $K = L, T, TL$  and  $TT$ , while the response functions defined in eq. (7) involve combinations of the form

$$w^{K'} \sim i(J^{\mu\dagger} J^\nu - J^{\nu\dagger} J^\mu) = -2(a^\mu \mathbf{b}^\nu - a^\nu \mathbf{b}^\mu + (\mathbf{b}^\mu \times \mathbf{b}^\nu)) \cdot \boldsymbol{\sigma}, \quad (56)$$

for  $K' = T', TL'$ . Therefore the single-nucleon responses  $w^K$  are proportional to the unit matrix in spin space and can be written as

$$w^K = w_S^K, \quad (57)$$

where the sub-index  $S$  means “scalar”, while the responses  $w^{K'}$  are proportional to the Pauli matrices and can be written as

$$w^{K'} = \mathbf{w}_V^{K'} \cdot \boldsymbol{\sigma}, \quad (58)$$

where the sub-index  $V$  means “vector”.



## 2.4.2 Momentum distribution of a shell

Remember that our initial nuclear state is a polarized one-hole state,

$$|A\rangle = \sum_{m_i} \mathcal{D}_{m_i i}^{(i)}(\Omega^*) b_{im_i}^\dagger |C\rangle, \quad (59)$$

while the final states of the residual nucleus involve two holes in the core,

$$|B\rangle = b_h^\dagger b_i^\dagger |C\rangle = |h^{-1}m_h, i^{-1}m'_i\rangle. \quad (60)$$

Following ref. [6] we introduce the scalar  $M^S$  and vector  $\mathbf{M}^V$  momentum distributions, defined by

$$n_B(\mathbf{p}) = \frac{1}{2}(M^S + \mathbf{M}^V \cdot \boldsymbol{\sigma}), \quad (61)$$

where now  $M^S$  and  $\mathbf{M}^V$  are independent of the spin indices. In order to compute these quantities, we must consider two cases, depending on the shell where the hole  $h$  is located.

In the first case we have  $h \neq i$  and obtain the unpolarized momentum distribution of a complete shell

$$n_B(\mathbf{p})_{rr'} = n_{rr'}^{(h)}(\mathbf{p})_{\text{unpol}} = \delta_{rr'} \frac{1}{8\pi} [j_h]^2 |\tilde{R}_h(p)|^2, \quad (62)$$

where

$$\tilde{R}_h(p) = \sqrt{\frac{2}{\pi}} \int_0^\infty dr r^2 j_h(pr) R_h(r) \quad (63)$$

is the radial wave function in momentum space. In this case we have for the scalar and vector momentum distributions:

$$M^S(\mathbf{p}) = \frac{1}{4\pi} [j_h]^2 |\tilde{R}_h(p)|^2, \quad \mathbf{M}^V(\mathbf{p}) = 0. \quad (64)$$

In the second case we have  $h = i$ . In appendix C we show that the momentum distribution of this shell is given by the momentum distribution of the complete (unpolarized) shell minus the (polarized) momentum distribution of the hole:

$$n_B(\mathbf{p})_{r'r} = n_{r'r}^{(i)}(\mathbf{p})_{\text{unpol}} - n_{r'r}^{(i)}(\mathbf{p}, \Omega^*)_{\text{hole}}, \quad (65)$$

where the scalar and vector momentum distributions for a hole are given by

$$M^S = 2 \sum_{\mathcal{J}} P_{\mathcal{J}}^+ f_{\mathcal{J}}^i A_{\mathcal{J}} [j_i]^2 |\tilde{R}_i(p)|^2 [Y_{\mathcal{J}}(\Omega^*) \otimes Y_{\mathcal{J}}(\hat{\mathbf{p}})]_{00} \quad (66)$$

$$M_{\alpha}^V = \frac{2}{\sqrt{3}} \sum_{\mathcal{J}} \sum_{\mathcal{J}'=\mathcal{J}\pm 1} P_{\mathcal{J}}^- f_{\mathcal{J}}^i A_{\mathcal{J}\mathcal{J}'} [j_i]^2 |\tilde{R}_i(p)|^2 [Y_{\mathcal{J}}(\Omega^*) \otimes Y_{\mathcal{J}'}(\hat{\mathbf{p}})]_{1\alpha} \quad (67)$$

and where  $\alpha = 0, \pm 1$  refers to the spherical components of the vector. In the above equations we use the definitions:

$$A_{\mathcal{J}} \equiv \frac{1}{2} (-1)^{j_i-1/2} \begin{pmatrix} j_i & j_i & \mathcal{J} \\ 1/2 & -1/2 & 0 \end{pmatrix} \quad (68)$$

$$A_{\mathcal{J},\mathcal{J}+1} \equiv \frac{2\kappa_i + \mathcal{J} + 1}{[\mathcal{J}]\sqrt{\mathcal{J} + 1}} A_{\mathcal{J}} \quad (69)$$

$$A_{\mathcal{J},\mathcal{J}-1} \equiv \frac{2\kappa_i - \mathcal{J}}{[\mathcal{J}]\sqrt{\mathcal{J}}} A_{\mathcal{J}} \quad (70)$$

and  $\kappa_i \equiv (-1)^{j_i+l_i+1/2} (j_i + 1/2)$ .

### 2.4.3 Expansions of the single-nucleon current and responses

For the single-nucleon current we follow the formalism of ref. [10]. There we perform an expansion of the on-shell relativistic electromagnetic single-nucleon current up to order  $\eta = p/M$ , but importantly do not expand on the dimensionless variables  $\kappa = q/2M$  and  $\lambda = \omega/2M$  as was usually done in the past. The expressions for the charge and transverse current spin-matrices introduced in eq. (50) are the following:

$$\rho(\mathbf{p}', \mathbf{p}) = \rho_c + i\rho_{so}(\cos\phi\sigma_y - \sin\phi\sigma_x)\delta \quad (71)$$

$$J^x(\mathbf{p}', \mathbf{p}) = iJ_m\sigma_y + J_c\delta\cos\phi \quad (72)$$

$$J^y(\mathbf{p}', \mathbf{p}) = -iJ_m\sigma_x + J_c\delta\sin\phi, \quad (73)$$

where the coordinate system is as in sect. 2.1,  $\delta = \eta \sin\theta$  is the variable used to label the order of the relativistic correction and  $(\theta, \phi)$  is the direction of  $\mathbf{p}$ . The factors  $\rho_c$  (charge),  $\rho_{so}$  (spin-orbit),  $J_m$  (magnetization) and  $J_c$  (convection) are

only  $(q, \omega)$ -dependent,

$$\rho_c = \frac{\kappa}{\sqrt{\tau}} G_E \quad (74)$$

$$\rho_{so} = \frac{2G_M - G_E \kappa}{\sqrt{1 + \tau}} \frac{\kappa}{2} \quad (75)$$

$$J_m = \sqrt{\tau} G_M \quad (76)$$

$$J_c = \frac{\sqrt{\tau}}{\kappa} G_E \quad (77)$$

and  $G_E, G_M$  are the electric and magnetic form factors of the nucleon for which we use the Galster parametrization [15].

Using these expansions and eqs. (55,56) we obtain the following expressions for the single-nucleon responses:

$$w^L = \rho_c^2 + \rho_{so}^2 \delta^2 \quad (78)$$

$$w^T = 2J_m^2 + J_c^2 \delta^2 \quad (79)$$

$$w^{TL} = 2\sqrt{2}(\rho_c J_c + \rho_{so} J_m) \delta \cos \phi \quad (80)$$

$$w^{TT} = -J_c^2 \delta^2 \cos 2\phi \quad (81)$$

$$w^{TL'} = 2\sqrt{2} \left[ \rho_c J_m \mathbf{e}_1 + J_c \rho_{so} \delta^2 \sin \phi (\cos \phi \mathbf{e}_2 - \sin \phi \mathbf{e}_1) - \rho_{so} J_m \delta \cos \phi \mathbf{e}_3 \right] \cdot \boldsymbol{\sigma} \quad (82)$$

$$w^{T'} = 2 \left[ J_c J_m \delta (\cos \phi \mathbf{e}_1 + \sin \phi \mathbf{e}_2) - J_m^2 \mathbf{e}_3 \right] \cdot \boldsymbol{\sigma} \quad (83)$$

As already noted, the  $w^K$  responses are spin independent, and all of the spin dependence goes into the  $w^{K'}$  responses.

#### 2.4.4 Inclusive nuclear responses

From eqs. (52), (57), (58) and (61) we can write the exclusive responses for a shell as

$$\mathcal{R}^K = Mp' w_S^K M^S(\mathbf{p}) \quad (84)$$

$$\mathcal{R}^{K'} = Mp' \mathbf{w}_V^{K'} \cdot \mathbf{M}^V(\mathbf{p}). \quad (85)$$

We obtain the inclusive responses for given proton and neutron shells by integration over the angles  $\Omega' = (\theta', \phi')$  of the outgoing nucleon. As the momentum density for a shell is a function of  $\mathbf{p} = \mathbf{p}' - \mathbf{q}$ , it is convenient to perform the integral using the variables  $(p, \phi)$  instead of  $\Omega'$ . Note that  $\phi' = \phi$  because we have chosen the  $z$ -axis along  $\mathbf{q}$  and that from  $p^2 = p'^2 + q^2 - 2p'q \cos \theta'$  we obtain  $d \cos \theta' = -pdp/p'q$ . Accordingly the inclusive responses of a shell can be written

$$R^K = \frac{M}{q} \int_{|p'-q|}^{p'+q} dp p \int_0^{2\pi} d\phi w_S^K M^S(\mathbf{p}) \quad (86)$$

$$R^{K'} = \frac{M}{q} \int_{|p'-q|}^{p'+q} dp p \int_0^{2\pi} d\phi \mathbf{w}_V^{K'} \cdot \mathbf{M}^V(\mathbf{p}) \quad (87)$$

For a complete (unpolarized) shell we have only the scalar momentum distribution; hence  $\mathbf{M}^V = 0$  and the  $T'$  and  $TL'$  responses are zero. From eq. (62) we see that  $M^S(\mathbf{p})$  depends only on  $p$ . The single-nucleon responses TL and TT in eqs. (80,81) are proportional to  $\cos \phi$  and  $\cos 2\phi$ , respectively, and therefore their contributions go away upon integration on  $\phi$  — as expected, a complete shell only has two inclusive responses  $L$  and  $T$ . In particular, for the expansions in eqs. (71-73) the only nonzero reduced responses are given by:

$$W_0^L = \frac{[j_i]}{4\pi} R^L = \frac{[j_i]}{2} \frac{M}{q} \int_{|p'-q|}^{p'+q} dp p (\rho_c^2 + \rho_{so}^2 \delta^2) M^S(p) \quad (88)$$

$$W_0^T = \frac{[j_i]}{4\pi} R^T = \frac{[j_i]}{2} \frac{M}{q} \int_{|p'-q|}^{p'+q} dp p (2J_m^2 + J_c^2 \delta^2) M^S(p). \quad (89)$$

From eq. (65) we see that the responses of a shell with a hole can be obtained as the response of the complete shell (given above) minus the response of a single hole. In appendix C we show that the reduced inclusive responses for a hole are given by

$$\left( W_{\mathcal{J}}^{K,K'} \right)_{\text{hole}} = -\frac{M}{q} \int_{|p'-q|}^{p'+q} dp p \frac{[j_i]}{4\pi} |\tilde{R}_i(p)|^2 \Phi_{\mathcal{J}}^{K,K'}(q, \omega, \cos \theta), \quad (90)$$

where the functions  $\Phi$  depend on  $p$  through the function

$$\cos \theta = (p'^2 - p^2 - q^2)/2pq \quad (91)$$

and they have the following forms to order  $\delta^2$ :

$$\Phi_{\mathcal{J}}^L = (\rho_c^2 + \rho_{so}^2 \delta^2) [\mathcal{J}] A_{\mathcal{J}} P_{\mathcal{J}}^0(\cos \theta) \quad (92)$$

$$\Phi_{\mathcal{J}}^T = (2J_m^2 + J_c^2 \delta^2) [\mathcal{J}] A_{\mathcal{J}} P_{\mathcal{J}}^0(\cos \theta) \quad (93)$$

$$\Phi_{\mathcal{J}}^{TL} = (\rho_c J_c + \rho_{so} J_m) \delta \frac{2\sqrt{2}[\mathcal{J}]}{\mathcal{J}(\mathcal{J}+1)} A_{\mathcal{J}} P_{\mathcal{J}}^1(\cos \theta) \quad (94)$$

$$\Phi_{\mathcal{J}}^{TT} = -J_c^2 \delta^2 \frac{[\mathcal{J}]}{(\mathcal{J}-1)_4} A_{\mathcal{J}} P_{\mathcal{J}}^2(\cos \theta) \quad (95)$$

$$\begin{aligned} \Phi_{\mathcal{J}}^{T'} &= 2J_m^2 \sum_{\mathcal{J}'=\mathcal{J}\pm 1} [\mathcal{J}][\mathcal{J}'] A_{\mathcal{J}\mathcal{J}'} \begin{pmatrix} \mathcal{J} & \mathcal{J}' & 1 \\ 0 & 0 & 0 \end{pmatrix} P_{\mathcal{J}'}^0(\cos \theta) \\ &+ J_c J_m \delta \sum_{\mathcal{J}'=\mathcal{J}\pm 1} \frac{2\sqrt{2}[\mathcal{J}][\mathcal{J}']}{\sqrt{\mathcal{J}'(\mathcal{J}'+1)}} A_{\mathcal{J}\mathcal{J}'} \begin{pmatrix} \mathcal{J} & \mathcal{J}' & 1 \\ 0 & 1 & -1 \end{pmatrix} P_{\mathcal{J}'}^1(\cos \theta) \end{aligned} \quad (96)$$

$$\begin{aligned} \Phi_{\mathcal{J}}^{TL'} &= \rho_c J_m \sum_{\mathcal{J}'=\mathcal{J}\pm 1} \frac{4[\mathcal{J}][\mathcal{J}']}{\sqrt{\mathcal{J}(\mathcal{J}+1)}} A_{\mathcal{J}\mathcal{J}'} \begin{pmatrix} \mathcal{J} & \mathcal{J}' & 1 \\ 1 & 0 & -1 \end{pmatrix} P_{\mathcal{J}'}^0(\cos \theta) \\ &- \rho_{so} J_m \delta \sum_{\mathcal{J}'=\mathcal{J}\pm 1} \frac{2\sqrt{2}[\mathcal{J}][\mathcal{J}'] A_{\mathcal{J}\mathcal{J}'}}{\sqrt{\mathcal{J}(\mathcal{J}+1)\mathcal{J}'(\mathcal{J}'+1)}} \begin{pmatrix} \mathcal{J} & \mathcal{J}' & 1 \\ 1 & -1 & 0 \end{pmatrix} P_{\mathcal{J}'}^1(\cos \theta) \\ &- \rho_{so} J_c \delta^2 \sum_{\mathcal{J}'=\mathcal{J}\pm 1} \frac{2\sqrt{2}[\mathcal{J}][\mathcal{J}'] A_{\mathcal{J}\mathcal{J}'}}{\sqrt{\mathcal{J}(\mathcal{J}+1)(\mathcal{J}'-1)_4}} \begin{pmatrix} \mathcal{J} & \mathcal{J}' & 1 \\ -1 & 2 & -1 \end{pmatrix} P_{\mathcal{J}'}^2(\cos \theta) \\ &- \rho_{so} J_c \delta^2 \sum_{\mathcal{J}'=\mathcal{J}\pm 1} \frac{2\sqrt{2}[\mathcal{J}][\mathcal{J}'] A_{\mathcal{J}\mathcal{J}'}}{\sqrt{\mathcal{J}(\mathcal{J}+1)}} \begin{pmatrix} \mathcal{J} & \mathcal{J}' & 1 \\ 1 & 0 & -1 \end{pmatrix} P_{\mathcal{J}'}^0(\cos \theta), \end{aligned} \quad (97)$$

with  $(\mathcal{J}-1)_4 \equiv (\mathcal{J}-1)\mathcal{J}(\mathcal{J}+1)(\mathcal{J}+2)$ . These equations are very useful to get a feeling about the size of the first- and second-order relativistic corrections in the responses, in contrast to the situation that occurs in the CSM where it is more difficult to know *a priori* the actual importance of the various orders. Note that in particular in the complete shell model calculation the contributions to order  $\delta$  and  $\delta^2$  cannot be independently separated in general. Moreover, it is also useful to compare with the results using the complete relativistic expressions for the single-nucleon responses in the factorized approximation. It is also very instructive, as we shall see in the next section, to compare these results with the ones obtained in the

CSM where the same expansion for the single-nucleon current operator is used.

The terms proportional to  $\delta^n$  in eqs. (92-97) will be of order  $\eta_F^n$  after integration over  $p$ , where  $p_F$  is some average nucleon momentum for the shell  $i$  (of order the Fermi momentum which implies that typically  $\eta_F$  will be of the order 1/4).

From eqs. (88,89) we see that in PWIA there are no first-order terms in  $\eta_F$  (there is no interference between charge and spin-orbit or between magnetization and convection pieces). Therefore the first relativistic correction to the static (longitudinal) charge and (transverse) spin responses is of  $O(\eta_F^2)$ , that is, very small as we shall see. The same considerations are applicable to the  $L$  and  $T$  responses for a hole.

As for the  $TL$  response, it is of  $O(\eta_F)$  and we see that the spin-orbit and convection contributions enter at the same level. Thus, at high  $q$  we expect that the effect of the spin-orbit term in this response (not included usually in non-relativistic calculations) has the same degree of importance as the convection current.

The  $TT$  response is of  $O(\eta_F^2)$ , explaining why it is always very small for quasielastic scattering. Strictly speaking we should neglect this contribution not only because it is small, but also because our expansion of the relativistic four-current has been truncated at  $O(\eta)$ . That is, to be consistent in computing the responses we should include only terms up to  $O(\eta)$ . However, it is useful to evaluate the  $O(\eta^2)$  effects even if incompletely to see whether or not they could have a significant impact on the  $TT$  response. Indeed, we shall see in the next section that this response is very sensitive to the distortion of the outgoing nucleon and therefore to details of the nuclear model.

The  $T'$  and  $TL'$  responses are of  $O(\eta_F^0)$  and so are expected to be larger than the  $TT$  and  $TL$  responses. The first-order correction to these responses is due to the spin-orbit piece in the  $TL'$  response and to the convection current contribution in the  $T'$  response.

## 3 Results

### 3.1 Comparisons of CSM and PWIA

Before showing results for more realistic nuclei, and in a first test of our formalism, it is useful to compare our model with an exactly soluble problem, namely, the simpler process of elastic scattering from a polarized proton at rest. Obviously, in that case the cross section is zero unless  $\omega = -Q^2/2M$ , implying that a factor  $\delta(\omega + Q^2/2M)$  appears in the responses. Aside from that factor, the polarized responses in this case are given by [1]:

$$W_0^L = (1 + \tau)G_E^2 \quad (98)$$

$$W_0^T = 2\tau G_M^2 \quad (99)$$

$$W_1^{TL'} = 2\sqrt{2}\sqrt{\tau(1 + \tau)}G_M G_E \quad (100)$$

$$W_1^{T'} = -2\tau G_M^2. \quad (101)$$

Here the initial spin is  $j_i = 1/2$  and we have only four responses corresponding to  $\mathcal{J} = 0, 1$ . Two are equal in magnitude,  $W_1^{T'} = -W_0^T$ , and inserting the typical value  $q = 500$  MeV/c we see that we have  $W_1^{TL'} \simeq 2W_0^L$ .

Now we compare these results with an extreme nuclear model that has one proton in the  $1s_{1/2}$  shell (actually we show the results for the well parameters of  $^{12}\text{C}$ , although the specific nucleus is not essential for the test). In this case we expect that the above elastic scattering results will be broadened in energy due to the momentum distribution of the proton, but that the integral over  $\omega$  of these responses approximately reproduces the elastic case. In particular, the relative order of magnitude of the different elastic responses seen above should be preserved, that is, the  $TL'$  response should be about two times the  $L$  response, while the  $T'$  responses should be about minus the  $T$  response. We can see in fig. 1 that these expectations are approximately met. Therein we show the different responses computed in the

CSM and PWIA (on-shell) in the solid and dashed curves, respectively. Although our purpose in this initial discussion is only to get a feeling for the qualitative behaviour of the responses, at this juncture we note already that the CSM and PWIA (on-shell) models give similar results, the most obvious difference being the clear energy shift that we discuss below. All of the responses seem to differ only by a scale factor, as do their integrals. The value of the  $L$  and  $TL'$  responses at the maximum are, respectively, about 0.3 and 0.6  $\text{GeV}^{-1}$ , while the  $T$  and  $T'$  ones take the values 0.3 and  $-0.3 \text{ GeV}^{-1}$ , respectively.

Thus, the structure for all of the polarized responses for a proton in the  $1s_{1/2}$  shell appears to be very easily accounted for, in contrast with the situation seen for nucleons in other shells. In particular, we display results in fig. 2 for a proton in the  $1p_{1/2}$  or  $2s_{1/2}$  shell, the one-hole nuclei  $^{15}\text{N}$  and  $^{31}\text{P}$  with well parameters taken from  $^{16}\text{O}$  and  $^{40}\text{Ca}$ , respectively, again total angular momentum 1/2 situations. Note that we do not really expect that the simple one-hole model should be very successful for mid-shell cases such as  $^{31}\text{P}$ ; it is used here mainly for illustrative purposes, although, as discussed below, polarized inclusive quasielastic electron scattering may provide a very powerful probe of configuration-mixing effects such as those expected for cases such as  $^{31}\text{P}$ . The  $1p_{1/2}$  and  $2s_{1/2}$  polarized responses obtained at a typical value of the momentum transfer  $q = 500 \text{ MeV}/c$  are shown in fig. 2. Here and in several of the cases to follow we omit the unpolarized responses  $W_0^{L,T}$ ; since these involve all of the nucleons, and not just the single valence particle carrying the nucleus' angular momentum in our extreme one-hole model, they behave rather similarly for all nuclei (compare, for instance, figs. 1 and 5 given below). Their magnitudes, of course, depend on factors that involve the charge  $Z$  and neutron number  $N$  of the given nucleus and their widths increase with Fermi momentum  $p_F$ . The polarized responses for the  $1s_{1/2}$  and  $2s_{1/2}$  cases, while differing in detail because they have different momentum distributions, are similar in magnitude and occur with the same signs. In contrast, the  $1p_{1/2}$  cases are rather different: first, their signs are usually the opposite from the  $s$ -wave cases and, second, the energy distributions now reflect



the  $p$ -wave nature of the momentum distribution. The signs in the  $p_{1/2}$  case are easily seen to arise from the fact that the total angular momentum is comprised of one unit of orbital angular momentum coupled with spin-1/2 in a “jack-knifed” configuration in which spin and total angular momentum projections oppose — said another way, if the total angular momentum is polarized in some given direction then the spin points in the same (opposite) direction for  $s_{1/2}$  ( $p_{1/2}$ ) states.

The PWIA (on-shell) formalism presented in the last section is very useful as it provides some insight into the behaviours observed for these special spin-1/2 cases. Starting with the  $s_{1/2}$  case, by using eqs. (96,97) for the leading-order dependences in the integrals in eq. (90) that determine the reduced responses in this model,

$$\Phi_1^{T'} = \frac{1}{\sqrt{2}} J_m^2, \quad \Phi_1^{TL'} = -\rho_c J_m, \quad (102)$$

we see that the integrands have no  $\theta$ -dependence. This is the same situation that occurs for the integrals in eqs. (88,89) for all unpolarized responses. These integrals are then simply of the form

$$W \propto \int_{|y|}^{2q+y} p dp \rho(p), \quad (103)$$

where  $\rho(p)$  is the appropriate momentum distribution ( $M^S(p)$  in the unpolarized cases and  $-|\tilde{R}_i(p)|^2$  for the  $s_{1/2}$  polarized cases; note that for these one-hole cases the minus sign of eq. (65) enters for the polarized responses). Here we have used an approximation for the limits of integration by neglecting binding effects — these are, of course, included in the actual results presented here — whereby  $p' \cong \sqrt{2M\omega(1 + \omega/2M)}$ , implying that  $p' - q \cong y$  with  $y$  the usual scaling variable (see ref. [16] and also several approximations discussed in ref. [17]). In the scaling limit where  $q \rightarrow \infty$  the upper limit may safely be taken to  $\infty$ , *i.e.*, larger than any characteristic nuclear momentum; on the other hand, the lower limit  $|y|$  determines how much of the relevant momentum distribution is integrated. When  $y = 0$  the full range of integration is covered and, as usual, the unpolarized responses attain

their maximum values, defining the quasielastic peak. In the cases of the  $2s$  polarized responses the situation is similar, except that only the valence (polarized) nucleon's momentum distribution enters. Starting from very low  $\omega$  ( $y < 0$ ) little of the momentum distribution is covered and the response is small. As  $\omega$  increases, the response also increases until the higher- $p$  part of  $|\tilde{R}_{2s}|^2$  is covered, “stalls” as the momentum integration passes through the node in the wave function ( $p \cong 120$  MeV/ $c$  which corresponds to  $\omega \cong 75$  and  $185$  MeV) and then increases again as the lower- $p$  part of the momentum distribution is covered. The quasielastic peak occurs as in the unpolarized situation near  $y = 0$  and then the pattern repeats as  $y$  continues to rise beyond zero. Consequently the  $2s$  polarized responses have the behaviour seen in fig. 2 with “shoulders” on the sides of the quasielastic peak. The fact that the response is not symmetrical reflects the behaviour of the single-nucleon form factors which vary with  $\omega$  through their dependences on  $|Q^2| = q^2 - \omega^2$ .

The polarized responses in the  $p_{1/2}$  case are a little more complicated in that the integrands in eq. (90) contain

$$\Phi_1^{T'} = \frac{1}{\sqrt{2}} J_m^2 \cos 2\theta, \quad \Phi_1^{TL'} = \rho_c J_m \cos^2 \theta \quad (104)$$

which have  $\theta$ -dependences through factors of  $\cos 2\theta$  and  $\cos^2 \theta$ , these in turn being functions of  $p$ ,  $q$  and  $y$  (see eq. (91)) through

$$\cos \theta = \frac{1}{2pq} (2qy + y^2 - p^2), \quad (105)$$

again neglecting binding effects for this argument. When  $p = |y|$ , one has  $\cos \theta = +1(-1)$  for  $y > 0(y < 0)$  and as  $p$  becomes larger  $|\cos \theta|$  falls off with characteristic half-width of  $2y$ . Thus, for very small  $y$  (near the quasielastic peak)  $|\cos \theta|$  is only large for a small region where  $p$  is close to  $|y|$ . This implies that the  $TL'$  response whose integral contains the factor  $\cos^2 \theta$  should be small, while the  $T'$  response, involving  $\cos 2\theta = 2 \cos^2 \theta - 1$ , should be large in magnitude, as observed in fig. 2. As  $|y|$  increases away from zero, the sampled region widens. In the  $TL'$  response the characteristic “double-bump” behaviour reflects the  $1p$  momentum distribution

where the peak positions are determined by the maximum in that distribution, namely about 100 MeV/c; in the  $T'$  response the factor  $\cos 2\theta$  changes sign as the integral progresses from  $p = |y|$  to higher values and accordingly can also produce a sign-change in the response itself.

Once the total angular momentum is 3/2 or larger the situation is clearly more complicated. Specifically, for  $j_i = 3/2$  one now has  $\mathcal{J} = 2$  and 3 (tensor- and octupole-polarized) responses in addition to  $\mathcal{J} = 0$  (unpolarized) and 1 (vector-polarized) responses. For a  $1p_{3/2}$  proton, corresponding to the one-hole nucleus  $^{11}\text{B}$  and using well parameters for  $^{12}\text{C}$ , we obtain the results shown in figs. 3 and 4 again for  $q = 500$  MeV/c (omitting the unpolarized responses for the reasons stated above). We observe first of all that in this “stretched” configuration (spin and orbital angular momentum projections in the same direction) the vector-polarized responses are again qualitatively the same as the  $s$ -wave cases discussed above. The tensor- and octupole-polarized responses, on the other hand, have no analogs in the spin-1/2 situations. These range in magnitude from being comparable to the vector-polarized responses ( $W_3^{T'}$ ) to being a factor of about two smaller ( $W_2^L, W_2^T, W_3^{TL'}$ ) to being more than an order of magnitude smaller ( $W_2^{TL}, W_2^{TT}$ ). The corresponding  $1d_{3/2}$  “jack-knifed” results, *i.e.*, for the case of  $^{39}\text{K}$ , are shown in figs. 5 and 6 (all of the responses are now given, since we shall return to discuss the results for this nucleus in more detail in the next two subsections). Here again the vector-polarized responses have the sign they do for the other “jack-knifed” case considered above, namely,  $1p_{1/2}$ . The magnitudes of the  $1d_{3/2}$  and  $1p_{3/2}$  are comparable, although, given the degree of structure observed, it is difficult to relate the results to any simple picture of the state occupied by the polarized nucleon.

The reason why the polarized unprimed responses are similar but the primed are so different for equal  $j_i$  and different  $l_i$  can be explained in PWIA. In fact, we see from eqs. (90,92-97) that the polarized unprimed responses depend on the orbital angular momentum  $l_i$  of the hole only via the momentum distribution  $|\tilde{R}_i(p)|^2$  of the

complete shell  $i$ . These distributions must satisfy the sum rule  $\int |\tilde{R}_i(p)|^2 = 1$  and thus we can suppose, as a first approximation that the integrals extend between the limits  $|p' - q|$  and  $p' + q$  for high  $q$  and are not very different for  $l_i = j_i \pm 1/2$ , so the quasielastic responses do not depend critically on  $l_i$ . Where the primed responses are concerned, we can see from eqs. (96,97) that they also depend on  $l_i$  via the coefficients  $A_{\mathcal{J}\mathcal{J}'}$  given in eqs. (69,70). As a consequence, the primed responses are very sensitive to the angular momentum  $l_i$  of the polarized shell.

Thus we see quite dramatically different behaviour when the quantum numbers of the nucleon carrying the polarization are varied. In a configuration-mixed situation such as occurs in the middle of the  $1p$ -shell we would expect that the polarization effects would arise from a combination of  $1p_{3/2}$  and  $1p_{1/2}$  contributions. Since the extreme, pure one-hole results presented here are so different for these two configurations, even changing sign, it is clear that the polarized responses have the potential to provide a sort of “configuration analyzer”. Another example is the  $^{31}\text{P}$  case introduced above, where we do not expect the pure  $2s_{1/2}$  proton hole model to be especially good and instead expect that configuration-mixing in the  $2s - 1d$  shell should be important. By examining, for instance, the vector polarized responses shown in the figures, it is again clear that the sensitivity to details of the configuration-mixing is high and that any significant deviation from the extreme  $2s_{1/2}$  results given in fig. 2 and  $1d_{3/2}$  results given in fig. 6 for  $W_1^{T',TL'}$  should be observable.

Let us now return to compare in more detail the results obtained for the two basic models considered in this work, the CSM and PWIA(on-shell) models; we return to make further connections with the PWIA(CC1) model at the beginning of the next subsection. We expect that the CSM predictions should be more representative of what will be measured when experiments are performed on polarized nuclei of the type we are considering in this work when the outgoing nucleon’s energy is relatively small, *i.e.*, when the momentum transfer and hence the energy transfer at

the quasielastic peak are relatively small. On the other hand, once the kinematics progress to the higher-energy regime, the FSI are expected to play a more minor role and the PWIA should be expected to become valid. We may take as “typical” regimes for the two situations conditions in which the outgoing nucleon is below say 50 MeV, where the FSI are surely quite strong and where (at least) the distortion effects included in the CSM treatment should be necessary, and at or above 200 MeV, where the real central nucleon-nucleus potential is known from optical model analyses of nucleon scattering to be rather small compared with its value at low or negative energies and thus where the PWIA should be adequate. From the relative simplicity of the PWIA formalism presented in this work it is clear that the latter when applicable has the advantage of providing a more direct connection to the desired initial-state nuclear structure issues. Part of our motivation in the present work is to assess the degree of sensitivity to FSI effects one should expect to see in the various inclusive polarized response functions through the use of the two extreme models.

Where the FSI distortion effects are concerned we have already seen above that the general behaviour of the responses in the CSM and PWIA models is similar (with the exception of the  $TT$  response that is discussed in more detail below). In particular, the Coulomb sum rule (the zeroth energy-weighted moment of  $W_0^L$  reduced in the standard way; see ref. [17]) is virtually the same and equal to unity in the two models for high momentum transfers. The plane-wave results are, on the average, shifted to the right with respect to the CSM responses. By forming the first energy-weighted sum rule [17] one sees that this shift is more or less constant as a function of  $q$ , whereas the width of the reduced response (the variance, see ref. [17]) is rather close to the same value in the two models.

The shift may be understood using the following argument: in the CSM the energy of the ejected nucleon  $\epsilon_p = t_p + v_p$  is the sum of kinetic plus potential energy, while in PWIA the energy of the nucleon  $\epsilon'_p = t'_p$  is only kinetic. As the two energies

are the same,  $\epsilon_p = \epsilon'_p$ , we have  $t'_p < t_p$  because the potential energy is negative. This means that the velocity of the nucleon knocked-out from the nuclear interior is greater for distorted than for plane waves, implying a shift of the responses. An alternative way of seeing this is the following: let us suppose that at high energy the matrix elements of the current computed in the PWIA or CSM are approximately the same,  $\langle J^\mu \rangle_{PW} \simeq \langle J^\mu \rangle_{CSM}$ , that the potential energy for the particle is a constant  $v_p \simeq -V < 0$ , and write  $t_p = \epsilon_p + V$ . Then we can write the PWIA hadronic tensor schematically as

$$\begin{aligned}
W_{PW}^{\mu\nu}(q, \omega) &= \sum \delta(t_p - \epsilon_h - \omega) \langle J^\mu \rangle_{PW}^* \langle J^\nu \rangle_{PW} \\
&\simeq \sum \delta(\epsilon_p + V - \epsilon_h - \omega) \langle J^\mu \rangle_{CSM}^* \langle J^\nu \rangle_{CSM} \\
&= W_{CSM}^{\mu\nu}(q, \omega - V).
\end{aligned} \tag{106}$$

This means that the PWIA responses will be shifted to the right of the CSM ones by an amount  $V$  which should arise as the average of the Woods-Saxon potential, in our case about  $\sim 30\text{--}35$  MeV, namely, approximately the order of the observed shifts.

Let us now return to a more detailed treatment of the case of  $^{39}\text{K}$  treated as a  $1d_{3/2}$  proton hole in closed shell  $^{40}\text{Ca}$  (for treatment of exclusive electron scattering from polarized  $^{39}\text{K}$  and  $^7\text{Li}$  see ref. [4]). In figs. 5 and 6 results were shown for  $q = 500$  MeV/c; now these are extended both to lower (300 MeV/c in figs. 7 and 8) and higher (700 MeV/c in figs. 9 and 10) momentum transfers. The naive quasielastic peak occurs at  $\omega = |Q^2|/2M = \sqrt{q^2 + M^2} - M$ , namely at  $\omega = 47, 125$  and  $232$  MeV for  $q = 300, 500$  and  $700$  MeV/c, respectively. Our expectation from the above arguments is thus that at 300 MeV/c the CSM should be more in accord with reality, since FSI should be strong at such low energies. In contrast, at 700 MeV/c at the quasielastic peak the outgoing nucleon is energetic enough that the FSI should be weak and the PWIA, not the CSM (which has the same potential acting in the final and initial states), should be more in line with the actual dynamics.

The results in figs. 5–10 show that, aside from the shift, the CSM and PWIA responses become rather similar at high momentum transfer, the exceptional case being the  $TT$  response. For low momentum transfer the basic structures still persist, although now some notable differences beyond a simple shift are observed; see for instance the  $W_1^{TL'}$ ,  $W_3^{T'}$  and  $W_3^{TL'}$  responses in fig. 8.

Now we discuss the  $TT$  response. This is the only case where the CSM and PWIA yield very different results for the structure and magnitude of the responses. The reason is the following: on the one hand, in PWIA the zeroth- and first-order terms in the expansion are exactly zero, due to cancelations in the spin sums, and consequently only the very small term involving the convection current survives. On the other hand, the terms that were exactly zero in PWIA are not zero for the CSM, because the radial wave function for an ejected nucleon with  $j = l + 1/2$  is slightly different from the  $j = l - 1/2$  one, due to the spin-orbit term in the Woods-Saxon potential, and thus the magnetization current gives some nonzero contribution; being of zeroth-order in  $\delta$ , it is enhanced with respect to the second-order contribution. As a consequence, the  $TT$  response could be interesting to exploit in studying distortion and shell effects, since in PWIA this response would be practically zero, but the FSI enhances the response by more than an order of magnitude at the maxima. Unfortunately, even with the distortion effects present as in the CSM this response is rather small and would likely be a challenge to measure.

The same argument could be applied to the  $TL$  responses, since in PWIA they have no zeroth-order contribution, but are of order  $O(\delta)$ . In this case it appears that the zeroth-order CSM contribution is the one responsible for the differences between the  $TL$  responses in PWIA and CSM, although in this case the effect is less pronounced; however, due to the larger values of these responses when compared with the  $TT$  cases, they might be better suited to measurement.

## 3.2 Relativistic corrections

In this subsection we briefly discuss some of the relativistic-order effects treated in the present work. We begin with a comparison of off-shell effects by comparing in fig. 11 the  $^{39}\text{K}$  even-rank responses at  $q = 500$  MeV/c for the PWIA (on-shell) — used in all other PWIA results given in this paper — and the PWIA (CC1), together with the CSM results again for reference. Specifically, for the off-shell model we use the  $CC1^{(0)}$  prescription discussed in ref. [5]. We see that typically the two PWIA models differ by a few and even up to about 10%, the exception again being the  $TT$  response which is very small in PWIA but where the on-/off-shell behaviour is most dramatic. In exploring the  $q$ -dependence of these differences (not shown) we find very little variation in going from 300 to 1000 MeV/c. Since we cannot know the correct form of the single-nucleon current, and must therefore take either model as being acceptable until off-shell effects can be better understood, these differences should be regarded as the scale of theoretical uncertainty stemming from nucleon model dependences — in fact, the uncertainties are representative only, since other models for off-shellness could yield still different results. In future work we intend to examine such behaviour in more depth.

The second aspect we want to comment upon refers to the expansion of the single-nucleon responses in powers of  $\delta = \eta \sin \theta$ . In the inclusive PWIA (on-shell) responses we have maintained these terms in order to be consistent with the shell model calculation, although clearly our treatment of second-order terms is incomplete since we have retained only contributions in the amplitudes of  $O(\delta)$  and then squared them, whereas other  $O(\delta^2)$  terms occur in the amplitudes themselves which can interfere with contributions of leading-order in another amplitude. We must not find large effects from this inconsistency or else we would have to question the entire procedure and indeed when comparing results with and without the second-order terms we find at most a few percent difference (excepting again the very small  $TT$  case). This is even smaller than the on-/off-shell differences discussed above and,



at least for inclusive quasielastic electron scattering if not necessarily elsewhere, can be safely ignored.

Finally, it is common in some non-relativistic quasielastic scattering calculations to omit the convection and (or) spin-orbit terms in the electromagnetic current. This is a good approximation for the unpolarized responses, but in the polarized case it is not so obvious that they can be ignored since there interferences occur that can enhance one or both of the terms. Accordingly we end our studies here with a discussion of the effects that are first-order in  $O(\delta)$ , focusing again on the case of  $^{39}\text{K}$  in the CSM. In figs. 12 and 13 we show results at  $q = 500$  MeV/c for the total current (solid curves), for the case where only the zeroth-order charge and magnetization terms have been retained (dashed curves) and for the case where charge, magnetization and convection terms are included (dot-dashed curves); only the total includes the spin-orbit contributions.

In PWIA the  $L$  and  $T$  responses have no first-order terms, and the only correction is of second-order. In contrast, in the CSM the first-order terms, while small, are not exactly zero. In the unpolarized  $L$  response the effect of the spin-orbit contribution is seen to be about 2.5% and grows to about 3% at 700 MeV/c and 4% at 1000 MeV/c. In the unpolarized  $T$  response the convection current produces less than 1.5% at 500 MeV/c, falls to below 1% at 700 MeV/c and continues to decrease with  $q$ , becoming entirely negligible at 1000 MeV/c. In both cases the other uncertainties are at least comparable, as discussed above.

This behaviour should be contrasted with the effects seen in the interference responses. In particular, as seen in eq. (94), the  $TL$  response is especially good when searching for first-order effects, since it is of first-order even in PWIA. Again, in contrast to the PWIA for the CSM the zeroth-order effects are nonzero, as seen in the dashed lines in fig. 12, although it is clear that first-order effects are also essential. By combining the results shown in fig. 12 for  $q = 500$  MeV/c with those shown in fig. 14 for  $q = 300$  and 700 MeV/c it is clear that the relative importance

of these effects does not go away with increasing momentum transfer, although the overall importance of this interference response function is not great and it may be difficult to isolate experimentally. In particular, we note in comparing the dot-dashed and solid curves that the effect of the spin-orbit terms, being proportional to the momentum transfer, becomes bigger at high  $q$ .

With regard to the (small)  $TT$  response, we see that zeroth-order effects are dominant while in PWIA they are zero, as discussed above. It is important to stress the fact that the dominance of zeroth-order effects arises exclusively from the distortion of the ejected nucleon.

Finally, from the eqs. (96,97) for the  $T'$  and  $TL'$  responses in PWIA we see that in fact here there are first-order terms that could be important. As seen in fig. 13 the  $T'$  response has relatively large convection current contributions that, as with the unpolarized  $T$  response discussed above, are large at low  $q$  and fall with increasing momentum transfer although still remaining non-negligible even at 1000 MeV/c. The  $TL'$  response, on the other hand is harder to analyze: for the PWIA the spin-orbit terms contribute in first order, whereas for the CSM both the spin-orbit and convection current terms can play a role. Again the effects seen here in the figure for 500 MeV/c are typical of what is found even at 1000 MeV/c.

## 4 Summary and conclusions

In this paper we have studied *inclusive* quasielastic scattering of polarized electrons from polarized nuclei, focusing on the six classes of response functions that occur,  $L$ ,  $T$ ,  $TL$ ,  $TT$  for situations where only the target is polarized and  $T'$  and  $TL'$  for situations having both polarized electrons and target nuclei. To illustrate the concepts involved we have obtained results in the extreme shell model for the case of one-hole nuclei employing the continuum shell model, on the one hand, and the plane-wave impulse approximation, on the other. Our expectation is that at

moderate momentum transfers, where the quasielastic peak lies at low energy and thus where the ejected nucleons are also low-energy, the CSM with the same potential in the initial and final states should fairly represent the mean-field interaction effects, whereas the PWIA, having no FSI will miss these effects insofar as the final state is concerned. In contrast, at high momentum transfers, where the quasielastic peak and outgoing nucleon energies are high, the FSI are expected to be rather weak and the PWIA should be applicable, whereas the CSM with the full potential (which is used in the present work to maintain orthogonality between initial and final single-particle wave functions) should exaggerate such effects.

Only one-body electromagnetic current operators are discussed in the present work, as these are expected to dominate in the quasifree regime considered, although in discussing the special interferences that occur in such polarization studies more work is needed to explore other effects that have been found to be small for unpolarized quasielastic scattering from medium nuclei, such as two-body meson-exchange currents [9]. In the polarization case such effects might be enhanced by interference with the one-body current, as happens for elastic scattering and electroexcitation of discrete states [18]. MEC effects have been explored in studies of high- $q$  quasi-free coincidence electron scattering, specifically for polarization transfer observables [19]. It is our intent to include such effects in treating inclusive polarization responses and to extend these studies to exclusive (polarized target) reactions in future work.

Drawing on our recent work [10] we use a new expansion in powers of  $p/M$  (up to first-order) for the on-shell nuclear electromagnetic current, that maintains all orders in  $q/M$  and  $\omega/M$  and, in addition, since we use relativistic kinematics in computing the momentum of the ejected nucleon, our approach incorporates several specific classes of relativistic contributions. These developments permit us to compute the responses at high momentum transfer and accordingly results are presented for the CSM and PWIA (on-shell) at  $q = 300\text{--}1000$  MeV/ $c$ . Comparisons have also been made for results in PWIA obtained with on- and off-shell single-nucleon currents.

In the present work our formalism has been applied to several selected nuclei containing a proton hole in a closed shell and special emphasis has been placed on  $^{39}\text{K}$ , being a good candidate for polarization measurements. Naturally it is straightforward to apply the same ideas to nuclei having a single proton above a closed shell and/or to odd-neutron cases; for brevity we have focused on proton hole examples. The study carried out for the selected nuclei shows that:

1. The PWIA responses are consistently similar to the CSM with the exception of a more or less constant shift to higher  $\omega$ , of the order of the nucleon binding energy, which arises since in PWIA the interaction energy of the ejected particle is neglected.
2. The results obtained in PWIA with on-shell and off-shell (CC1) single-nucleon currents do not differ significantly, usually falling at the few percent level except in a few cases where 10% is reached. This sets a scale of “theoretical uncertainty” for the other effects studies — clearly differences found to be at the few percent level would presently be hard to interpret.
3. The first-order (convection and spin-orbit) terms of the electromagnetic current play an important role in the  $TL$  response, while they fall typically at the few percent level for the other responses (excepting the  $TT$  response, see below). Given the inevitable uncertainties arising from on-/off-shell ambiguities, these few percent first-order effects will be hard to isolate. The  $TL$  response, however, has large enough first-order effects to make it a good candidate for such studies; in addition this response also shows measurable distortion effects.
4. Second-order terms in the responses are very small, suggesting that the first-order truncation in our formalism is more than sufficient for the typical momenta involved.
5. The unprimed responses  $L$ ,  $T$ ,  $TL$  and  $TT$  are not very sensitive to the value of the orbital angular momentum  $l$  of the hole shell, and they only depend of

the value of  $j$ . In contrast, the primed responses  $T'$  and  $TL'$  present different structures for different  $l$ 's and equal  $j$ .

6. The  $TT$  response is compatible with zero in PWIA, because it is of second-order in  $p/M$ ; however, it is considerably enhanced by distortion effects, since the zeroth-order terms are nonzero in the CSM. Thus, while small, this response is quite sensitive to details in the nuclear model of the reaction.

In summary, in contrast to the traditional unpolarized quasielastic responses where distortion and first-order current terms are not very important (except that the former produces an overall shift in energy), we have shown that these are in some cases essential for a proper description of the polarized inclusive nuclear responses. Of special interest for nuclear structure studies is the dramatic behaviour seen for the odd-rank  $T'$  and  $TL'$  polarized responses when different single-particle orbits are involved. Clearly when the nuclear ground state is not a one-hole configuration, but has other multi-particle-hole states mixed in, shells other than that at the Fermi surface may play a role. The fact that the polarized responses display very large sensitivity, even changing sign in some cases such as in going from  $1p_{3/2}$  to  $1p_{1/2}$ , suggests that inclusive polarized quasielastic electron scattering at relatively high momentum transfers may provide an excellent tool for studies of near-valence nucleon momentum distributions.

# Appendices

## A Reduced responses for a hole nucleus

In this appendix we show how to perform the sums over the angular momenta of the residual nucleus,  $J_B$ , and final state,  $j_f$ , in the reduced responses for a nucleus whose ground state can be described by as an extreme one-hole configuration. In the calculation of particle-hole excitations we must consider two kinds of contributions, those with two holes in different shells of the core,  $h \neq i$ , and those with  $h = i$ ; the second is the relevant one for the polarization observables, as we shall see below. In general the final state may be written

$$|f\rangle = \left\{ (1 - \delta_{hi})[a_p^\dagger [b_h^\dagger b_i^\dagger]_{J_B}]_{j_f} + \delta_{hi} \frac{1}{\sqrt{2}} [a_p^\dagger [b_i^\dagger b_i^\dagger]_{J_B}]_{j_f} \right\} |C\rangle, \quad (107)$$

where in the  $h = i$  term one has  $J_B = \text{even}$ , since there are two fermions (holes) in the same shell. The reduced matrix element of a multipole operator  $\hat{T}_J$  is then given by

$$\begin{aligned} \langle f || \hat{T}_J || A \rangle &= [J_B][j_f] (-1)^{J+j_p+j_h} \left\{ \begin{array}{ccc} j_i & j_f & J \\ j_p & j_h & J_B \end{array} \right\} \\ &\times \left\{ (1 - \delta_{hi}) \langle p || T_J || h \rangle + \sqrt{2} \delta_{hi} \langle p || T_J || i \rangle \right\}. \end{aligned} \quad (108)$$

We write the reduced response functions  $W_{\mathcal{J}}^K$ ,  $K = L, T, \dots$ , in the shell model as sums over responses for each hole  $h$ :

$$W_{\mathcal{J}}^K = \sum_h W_{\mathcal{J}h}^K, \quad (109)$$

and since the following procedures are analogous for each one of the six responses, we illustrate the steps only for the longitudinal case.

## A.1 Reduced responses for $h \neq i$

In the case  $h \neq i$  we write for eq. (25)

$$W_{\mathcal{J}h}^L = \sum_p \delta(\epsilon_p - \epsilon_h - \omega) \sum_{JJ'} [J][J'] [\mathcal{J}] \xi_{J',J}^+ \begin{pmatrix} J' & J & \mathcal{J} \\ 0 & 0 & 0 \end{pmatrix} u_{J',Jph}^L, \quad (110)$$

where we have defined

$$\begin{aligned} u_{J',Jph}^L &\equiv \sum_{j_f J_B} (-1)^{j_i+j_f} \begin{Bmatrix} J' & J & \mathcal{J} \\ j_i & j_i & j_f \end{Bmatrix} \langle p, (hi)_{J_B}; j_f \| \hat{M}_{J'} \| A \rangle \langle p, (hi)_{J_B}; j_f \| \hat{M}_J \| A \rangle \\ &= \sum_{j_f} (-1)^{j_i+j_f} [j_f]^2 \begin{Bmatrix} J' & J & \mathcal{J} \\ j_i & j_i & j_f \end{Bmatrix} t_{CJ'} t_{CJ} \\ &\quad \times \sum_{J_B} [J_B]^2 \begin{Bmatrix} j_i & j_f & J' \\ j_p & j_h & J_B \end{Bmatrix} \begin{Bmatrix} j_i & j_f & J \\ j_p & j_h & J_B \end{Bmatrix}. \end{aligned} \quad (111)$$

Here  $t_{CJ} = \langle p \| M_J \| h \rangle$  is the Coulomb multipole for the single-particle-hole excitation. Using the orthogonality of the 6-j symbols the last summation yields  $\delta_{JJ'} \frac{1}{[J]^2}$  and hence

$$u_{J',Jph}^L = \delta_{JJ'} \sum_{j_f} (-1)^{j_i+j_f} \begin{Bmatrix} J' & J & \mathcal{J} \\ j_i & j_i & j_f \end{Bmatrix} \frac{[j_f]^2}{[J]^2} t_{CJ}^2. \quad (112)$$

We can also perform the sum over  $j_f$  using

$$\sum_{j_f} (-1)^{j_i+j_f} \begin{Bmatrix} J' & J & \mathcal{J} \\ j_i & j_i & j_f \end{Bmatrix} [j_f]^2 = \delta_{\mathcal{J}0} (-1)^J [J] [j_i] \quad (113)$$

and therefore obtain

$$u_{J',Jph}^L = \delta_{JJ'} \delta_{\mathcal{J}0} (-1)^J \frac{[j_i]}{[J]} t_{CJ}^2. \quad (114)$$

Evaluating the 3-j symbol in eq. (110) for  $\mathcal{J} = 0$  we obtain the required result for the  $h \neq i$  case:

$$W_{\mathcal{J}h}^L = \delta_{\mathcal{J}0} [j_i] \sum_{pJ} \delta(\epsilon_p - \epsilon_h - \omega) t_{CJ}^2. \quad (115)$$

The same procedure may be followed for the other responses: in each instance one first sums over  $J_B$ , getting  $J = J'$ , and then sums over  $j_f$  obtaining a factor  $\delta_{\mathcal{J}0}$ . Since  $\mathcal{J} = 0$  corresponds to the unpolarized result (*i.e.*, only  $f_0^i$  occurs in eqs. (19–24)), no polarization dependence arises from the closed shell, as expected.

## A.2 Reduced responses for $h = i$

In this case the procedure is similar, although now we do not obtain  $J = J'$  because the only allowed values for  $J_B$  are even. In particular, for the longitudinal response we have

$$u_{J'Jpi}^L = \sum_{j_f} (-1)^{j_i+j_f} \left\{ \begin{matrix} J' & J & \mathcal{J} \\ j_i & j_i & j_f \end{matrix} \right\} t_{CJ'} t_{CJ} \\ \times \sum_{J_B=\text{even}} 2[J_B]^2 [j_f]^2 \left\{ \begin{matrix} j_i & j_f & J' \\ j_p & j_i & J_B \end{matrix} \right\} \left\{ \begin{matrix} j_i & j_f & J \\ j_p & j_i & J_B \end{matrix} \right\}, \quad (116)$$

where now  $t_{CJ} = \langle p || M_J || i \rangle$ . The sum over  $J_B$  in this case (see eqs. (6.2.9) and (6.2.11) in ref. [11]) gives  $\frac{\delta_{JJ'}}{[J]^2} - (-1)^{2j_i+J'+J} \left\{ \begin{matrix} j_i & j_f & J \\ j_i & j_p & J' \end{matrix} \right\}$ . The  $\delta_{JJ'}$  term just gives the same result as above and corresponds to the unpolarized reduced response of the complete shell  $i$ ; the term with the 6-j is the only one that contributes to the polarization observables. We find

$$u_{J'Jpi}^L = \delta_{JJ'} \delta_{\mathcal{J}0} (-1)^J \frac{[j_i]}{[J]} t_{CJ}^2 \\ + \sum_{j_f} (-1)^{j_i+j_f} \left\{ \begin{matrix} J' & J & \mathcal{J} \\ j_i & j_i & j_f \end{matrix} \right\} (-1)^{J'+J} [j_f]^2 \left\{ \begin{matrix} j_i & j_f & J \\ j_i & j_p & J' \end{matrix} \right\} t_{CJ'} t_{CJ}. \quad (117)$$

For the second term here we use eq. (6.2.11) in ref. [11],

$$\sum_{j_f} (-1)^{j_i+j_f} [j_f]^2 \left\{ \begin{matrix} J' & J & \mathcal{J} \\ j_i & j_i & j_f \end{matrix} \right\} \left\{ \begin{matrix} j_i & j_f & J \\ j_i & j_p & J' \end{matrix} \right\} = (-1)^{j_i-\mathcal{J}-j_p} \left\{ \begin{matrix} J' & J & \mathcal{J} \\ j_i & j_i & j_p \end{matrix} \right\}, \quad (118)$$

yielding

$$u_{J'Jpi}^L = \delta_{JJ'} \delta_{\mathcal{J}0} (-1)^J \frac{[j_i]}{[J]} t_{CJ}^2 \\ - (-1)^{j_i+j_p} (-1)^{J+J'+\mathcal{J}} \left\{ \begin{matrix} J' & J & \mathcal{J} \\ j_i & j_i & j_p \end{matrix} \right\} t_{CJ'} t_{CJ}. \quad (119)$$



Finally, the total longitudinal reduced response can be cast in the form

$$\begin{aligned}
W_{\mathcal{J}i}^L &= \delta_{\mathcal{J}0}[j_i] \sum_{pJ} \delta(\epsilon_p - \epsilon_i - \omega) t_{CJ}^2 \\
&- \sum_{pJJ'} \delta(\epsilon_p - \epsilon_i - \omega) (-1)^{j_i+j_p+\mathcal{J}} [J][J'][\mathcal{J}] \\
&\quad \times \begin{pmatrix} J' & J & \mathcal{J} \\ 0 & 0 & 0 \end{pmatrix} \left\{ \begin{matrix} J' & J & \mathcal{J} \\ j_i & j_i & j_p \end{matrix} \right\} \xi_{JJ'}^+ t t_{CJ'} t_{CJ}, \quad (120)
\end{aligned}$$

with similar results for  $T$ ,  $TL$ , *etc.*

## B Multipoles of the spin-orbit charge density

Here we present the formalism used in the computation of the Coulomb reduced matrix elements of the spin-orbit term. We begin with the matrix element of the spin-orbit charge density operator (see ref. [10]) between nucleon plane-wave states,

$$\langle \mathbf{p}'s' | \rho_{so}(\mathbf{q}, \omega) | \mathbf{p}, s \rangle = \delta(\mathbf{p} + \mathbf{q} - \mathbf{p}') \frac{2G_M - G_E}{\sqrt{1 + \tau}} \frac{i}{4M^2} (\mathbf{q} \times \mathbf{p}) \cdot \boldsymbol{\sigma}_{s's}. \quad (121)$$

It is convenient to define a “bare” operator  $\bar{\rho}_{so}$  extracting the form factor  $2G_M - G_E$  and the kinematical factor  $\sqrt{1 + \tau}$ :

$$\rho_{so}(\mathbf{q}) \equiv \frac{2G_M - G_E}{\sqrt{1 + \tau}} \bar{\rho}_{so}(\mathbf{q}) \quad (122)$$

$$\langle \mathbf{p}'s' | \bar{\rho}_{so}(\mathbf{q}) | \mathbf{p}, s \rangle = \delta(\mathbf{p} + \mathbf{q} - \mathbf{p}') \frac{i}{4M^2} (\mathbf{q} \times \mathbf{p}) \cdot \boldsymbol{\sigma}_{s's}, \quad (123)$$

where now  $\bar{\rho}_{so}$  is independent of the energy transfer  $\omega$ . The coordinate-space expression for this operator is

$$\bar{\rho}_{so}(\mathbf{r}) = \frac{i}{8M^2} \nabla \times [\delta(\mathbf{r} - \mathbf{r}_1) \nabla_1 + \nabla_1 \delta(\mathbf{r} - \mathbf{r}_1)] \cdot \boldsymbol{\sigma}, \quad (124)$$

where  $\mathbf{r}_1$  denotes the position operator of the nucleon and  $-i\nabla_1 = \mathbf{p}_1$  its momentum operator. The symmetrized form  $i(\delta\nabla + \nabla\delta)$  ensures the hermiticity of the operator.

The Coulomb multipole operator for the spin-orbit charge density is written

$$M_{JM}(q) = \frac{2G_M - G_E}{\sqrt{1 + \tau}} \overline{M}_{JM}(q), \quad (125)$$

where the “bare” multipole operator  $\overline{M}_{JM}(q)$  is defined from the “bare” charge-density  $\overline{\rho}_{so}$  in the usual way

$$\overline{M}_{JM}(q) = \int d^3r j_J(qr) Y_{JM}(\hat{\mathbf{r}}) \overline{\rho}_{so}(\mathbf{r}). \quad (126)$$

Inserting the coordinate-space expression for  $\overline{\rho}_{so}$  we obtain

$$\overline{M}_{JM}(q) = -\frac{i}{4M^2} [\nabla_1 j_J(qr_1) Y_{JM}(\hat{\mathbf{r}}_1)] \times \nabla_1 \cdot \boldsymbol{\sigma}, \quad (127)$$

where the first gradient  $\nabla_1$  only operates on the functions within the brackets. For simplicity, in the following we shall call  $\mathbf{r}$  the coordinate of the nucleon (instead of  $\mathbf{r}_1$ ). The gradient of a spherical Bessel function times a spherical harmonic may be expressed in terms of vector spherical harmonics (see eq. (5.9.17) in ref. [11]), yielding

$$\overline{M}_{JM}(q) = -\frac{i}{4M^2} \frac{q}{[J]} \sum_{s=\pm 1} \sqrt{J + \delta_{s1}} j_{J'}(qr) [\mathbf{Y}_{J'JM}(\hat{\mathbf{r}}) \times \nabla] \cdot \boldsymbol{\sigma}, \quad (128)$$

where  $J' = J + s$  and as usual  $[J] = \sqrt{2J + 1}$ .

In order to compute the reduced matrix elements of the Coulomb multipole operator  $\overline{M}_{JM}$ , it is convenient to write it as a linear combination of the basic irreducible tensor operators

$$\mathcal{D}_{J'LM} \equiv [[Y_{J'}(\hat{\mathbf{r}}) \otimes \nabla]_L \otimes \sigma]_{JM}. \quad (129)$$

To this end we use the facts that for any vector operator  $\mathbf{A}$  one has  $\mathbf{Y}_{LJM} \cdot \mathbf{A} = [Y_L \otimes A]_{JM}$  and for any two vector operators  $\mathbf{A}$  and  $\mathbf{B}$  one has  $(\mathbf{A} \times \mathbf{B})_\alpha = -i\sqrt{2}[A \otimes B]_{1\alpha}$ . One then has

$$[\mathbf{Y}_{J'JM} \times \nabla] \cdot \boldsymbol{\sigma} = \mathbf{Y}_{J'JM} \cdot [\nabla \times \boldsymbol{\sigma}] = -i\sqrt{2} [Y_{J'} \otimes [\nabla \otimes \sigma]_1]_{JM}, \quad (130)$$

or, using a 6-j symbol to recouple the angular momenta, one has

$$[\mathbf{Y}_{J'JM} \times \nabla] \cdot \boldsymbol{\sigma} = i\sqrt{6} \sum_L [L] \left\{ \begin{array}{ccc} J' & 1 & L \\ 1 & J & 1 \end{array} \right\} [[Y_{J'} \otimes \nabla]_L \otimes \sigma]_{JM}. \quad (131)$$

Inserting this expression in eq. (128) we obtain

$$\overline{M}_{JM}(q) = \frac{\sqrt{6}}{4M^2} \frac{q}{[J]} \sum_{s=\pm 1} \sqrt{J + \delta_{s1}} S_{J'JM}(q), \quad (132)$$

where the operator  $S_{J'JM}(q)$  is defined as

$$S_{J'JM}(q) \equiv \sum_{L=J,J'} [L] \left\{ \begin{array}{ccc} J' & 1 & L \\ 1 & J & 1 \end{array} \right\} j_{J'}(qr) \mathcal{D}_{J'LJM}. \quad (133)$$

Note that the sum over  $L$  has only two nonzero terms,  $L = J, J'$ , because the two triangle relations  $J-1 \leq L \leq J+1$  and  $J'-1 \leq L \leq J'+1$  must hold simultaneously.

In evaluating the matrix elements of  $S_{J'JM}(q)$  it is useful to treat spin, orbital angular momentum and radial dependences separately, since our single-particle wave functions are labeled  $|p\rangle = |n_p \frac{1}{2} l_p; j_p m_p\rangle$ . We must compute the reduced matrix element taken between particle and hole states:

$$\langle p || S_{J'JM}(q) || h \rangle = \sum_{L=J,J'} [L] \left\{ \begin{array}{ccc} J' & 1 & L \\ 1 & J & 1 \end{array} \right\} \langle p || j_{J'}(qr) \mathcal{D}_{J'LJ} || h \rangle. \quad (134)$$

The spin reduced matrix element is given by  $\langle \frac{1}{2} || \sigma || \frac{1}{2} \rangle = \sqrt{6}$  and for the angular reduced matrix element we have

$$\begin{aligned} \langle l_p || [Y_{J'} \otimes \nabla]_L || l_h \rangle &= \frac{(-)^{l_h+L}}{\sqrt{4\pi}} [L][l_p][J'] \sum_{s_h=\pm 1} s_h \sqrt{l_h + \delta_{s_h,1}} [L_h] \left\{ \begin{array}{ccc} J' & 1 & L \\ l_h & l_p & L_h \end{array} \right\} \\ &\times \begin{pmatrix} L_h & J' & l_p \\ 0 & 0 & 0 \end{pmatrix} \left( \frac{d}{dr} - s_h \frac{l_h + \delta_{s_h,-1}}{r} \right), \end{aligned} \quad (135)$$

defining  $L_h = l_h + s_h$  and using the fact that

$$\langle l || \nabla || l_h \rangle = \sum_{s_h=\pm 1} s_h \sqrt{l_h + \delta_{s_h,1}} \delta_{lL_h} \left( \frac{d}{dr} - s_h \frac{l_h + \delta_{s_h,-1}}{r} \right) \quad (136)$$

together with eqs. (5.4.5) and (7.1.1) in ref. [11]. Using this result we arrive at the following expression for the required matrix elements:

$$\begin{aligned}
\langle p || j_{J'} \mathcal{D}_{J' L J} || h \rangle &= (-)^{l_h + J + 1} [j_p][j_h][J][J'][L][l_p] \frac{\sqrt{6}}{\sqrt{4\pi}} \begin{Bmatrix} \frac{1}{2} & l_p & j_p \\ \frac{1}{2} & l_h & j_h \\ 1 & L & J \end{Bmatrix} \\
&\times \sum_{s_h = \pm 1} s_h \sqrt{l_h + \delta_{s_h, -1}} [L_h] \begin{Bmatrix} J' & 1 & L \\ l_h & l_p & L_h \end{Bmatrix} \begin{pmatrix} L_h & J' & l_p \\ 0 & 0 & 0 \end{pmatrix} \\
&\times \int_0^\infty dr r^2 R_p j_{J'}(qr) \left( \frac{d}{dr} - s_h \frac{l_h + \delta_{s_h, -1}}{r} \right) R_h, \quad (137)
\end{aligned}$$

where  $R_p(r)$  and  $R_h(r)$  are the radial wave functions. Making explicit the sum over  $L$ , the matrix element in eq. (134) then becomes

$$\begin{aligned}
\langle p || S_{J' J M}(q) || h \rangle &= \\
&[J] \begin{Bmatrix} J' & 1 & J \\ 1 & J & 1 \end{Bmatrix} (-)^{l_h + J + 1} [j_p][j_h][J][J'][J][l_p] \frac{\sqrt{6}}{\sqrt{4\pi}} \begin{Bmatrix} \frac{1}{2} & l_p & j_p \\ \frac{1}{2} & l_h & j_h \\ 1 & J & J \end{Bmatrix} \\
&\times \sum_{s_h = \pm 1} s_h \sqrt{l_h + \delta_{s_h, -1}} [L_h] \begin{Bmatrix} J' & 1 & J \\ l_h & l_p & L_h \end{Bmatrix} \begin{pmatrix} L_h & J' & l_p \\ 0 & 0 & 0 \end{pmatrix} \\
&\times \int_0^\infty dr r^2 R_p j_{J'}(qr) \left( \frac{d}{dr} - s_h \frac{l_h + \delta_{s_h, -1}}{r} \right) R_h \\
&+ [J'] \begin{Bmatrix} J' & 1 & J' \\ 1 & J & 1 \end{Bmatrix} (-)^{l_h + J + 1} [j_p][j_h][J][J'][J][l_p] \frac{\sqrt{6}}{\sqrt{4\pi}} \begin{Bmatrix} \frac{1}{2} & l_p & j_p \\ \frac{1}{2} & l_h & j_h \\ 1 & J' & J \end{Bmatrix} \\
&\times \sum_{s_h = \pm 1} s_h \sqrt{l_h + \delta_{s_h, -1}} [L_h] \begin{Bmatrix} J' & 1 & J' \\ l_h & l_p & L_h \end{Bmatrix} \begin{pmatrix} L_h & J' & l_p \\ 0 & 0 & 0 \end{pmatrix} \\
&\times \int_0^\infty dr r^2 R_p j_{J'}(qr) \left( \frac{d}{dr} - s_h \frac{l_h + \delta_{s_h, -1}}{r} \right) R_h. \quad (138)
\end{aligned}$$

Moreover, the product of a 6- $j$  with the 3- $j$  can be evaluated using

$$\begin{Bmatrix} J' & 1 & J \\ l_h & l_p & L_h \end{Bmatrix} \begin{pmatrix} L_h & J' & l_p \\ 0 & 0 & 0 \end{pmatrix} =$$

$$\begin{aligned} & \frac{P_{l_p+l_h+J}^+}{[L_h][l_h][J][J']} \left\{ [(l_h + \delta_{s_h,-1})(J + \delta_{s,-1})]^{1/2} \begin{pmatrix} l_h & J & l_p \\ 1 & -1 & 0 \end{pmatrix} \right. \\ & \left. - s_h s [(l_h + \delta_{s_h,1})(J + \delta_{s,1})]^{1/2} \begin{pmatrix} l_h & J & l_p \\ 0 & 0 & 0 \end{pmatrix} \right\} \end{aligned} \quad (139)$$

$$\begin{pmatrix} J' & 1 & J' \\ l_h & l_p & L_h \end{pmatrix} \begin{pmatrix} L_h & J' & l_p \\ 0 & 0 & 0 \end{pmatrix} = \frac{P_{l_p+l_h+J}^+}{[L_h][l_h][J']} (l_h + \delta_{s_h,-1})^{1/2} \begin{pmatrix} l_h & J' & l_p \\ 1 & -1 & 0 \end{pmatrix}. \quad (140)$$

We may then perform the sums over  $s_h$  and, after some algebra, write the matrix element in the following way:

$$\begin{aligned} \langle p || S_{J'J}(q) || h \rangle &= A_{J'J}(ph) \int_0^\infty dr r R_p(r) j_{J'}(qr) R_h(r) \\ &+ B_{J'J}(ph) \int_0^\infty dr r^2 R_p(r) j_{J'}(qr) \frac{dR_h}{dr}, \end{aligned} \quad (141)$$

where we have defined the coupling factors:

$$\begin{aligned} A_{J'J}(ph) &= P_{l_p+l_h+J}^+ a_{phJ} [J] \sqrt{(J + \delta_{s,-1}) l_h (l_h + 1)} \\ &\times \begin{pmatrix} J' & 1 & J \\ 1 & J & 1 \end{pmatrix} \begin{pmatrix} \frac{1}{2} & l_p & j_p \\ \frac{1}{2} & l_h & j_h \\ 1 & J & J \end{pmatrix} \begin{pmatrix} l_h & J & l_p \\ 1 & -1 & 0 \end{pmatrix} \\ &+ P_{l_p+l_h+J}^+ a_{phJ} [J']^2 \sqrt{l_h (l_h + 1)} \\ &\times \begin{pmatrix} J' & 1 & J' \\ 1 & J & 1 \end{pmatrix} \begin{pmatrix} \frac{1}{2} & l_p & j_p \\ \frac{1}{2} & l_h & j_h \\ 1 & J' & J \end{pmatrix} \begin{pmatrix} l_h & J' & l_p \\ 1 & -1 & 0 \end{pmatrix} \end{aligned} \quad (142)$$

$$\begin{aligned} B_{J'J}(ph) &= P_{l_p+l_h+J}^+ a_{phJ} [J] s \sqrt{J + \delta_{s,1}} \\ &\times \begin{pmatrix} J' & 1 & J \\ 1 & J & 1 \end{pmatrix} \begin{pmatrix} \frac{1}{2} & l_p & j_p \\ \frac{1}{2} & l_h & j_h \\ 1 & J & J \end{pmatrix} \begin{pmatrix} l_h & J & l_p \\ 0 & 0 & 0 \end{pmatrix} \end{aligned} \quad (143)$$

with

$$a_{phJ} \equiv \sqrt{\frac{3}{2\pi}} (-1)^{l_p} [l_p][l_h][j_p][j_h][J]. \quad (144)$$

These lead to the required matrix elements of the Coulomb operator  $\overline{M}_J$ :

$$\langle p | \overline{M}_J(q) | h \rangle = \frac{\sqrt{6}}{4M^2} \frac{q}{[J]} \left[ \sqrt{J} \langle p | S_{J-1,J}(q) | h \rangle + \sqrt{J+1} \langle p | S_{J+1,J}(q) | h \rangle \right]. \quad (145)$$

Finally, we note the following useful identities to assist in computing quasielastic responses where the sums over multipoles involve large numbers of coupling coefficients. To speed up the calculation it is convenient to reduce the order of the  $n$ - $j$  coefficients whenever possible employing the following:

$$\left\{ \begin{array}{ccc} \frac{1}{2} & l_p & j_p \\ \frac{1}{2} & l_h & j_h \\ 1 & J & J \end{array} \right\} \left( \begin{array}{ccc} l_h & J & l_p \\ 0 & 0 & 0 \end{array} \right) = P_{l_p+l_h+J}^+ \frac{(-1)^{j_p+l_p-1/2}}{\sqrt{6}[l_p][l_h][J]} \frac{\kappa_p - \kappa_h}{\sqrt{J(J+1)}} \left( \begin{array}{ccc} j_p & j_h & J \\ -\frac{1}{2} & \frac{1}{2} & 0 \end{array} \right) \quad (146)$$

$$\left\{ \begin{array}{ccc} \frac{1}{2} & l_p & j_p \\ \frac{1}{2} & l_h & j_h \\ 1 & J & J \end{array} \right\} \left( \begin{array}{ccc} l_h & J & l_p \\ 1 & -1 & 0 \end{array} \right) = \frac{1}{2\sqrt{6}[l_p][l_h][J]} \left\{ \left[ \frac{\kappa_h + 1}{\kappa_h} \right]^{1/2} \left( \begin{array}{ccc} j_h & j_p & J \\ -\frac{1}{2} & \frac{1}{2} & 0 \end{array} \right) \right. \\ + \frac{(-1)^{j_p+l_p+1/2}}{\sqrt{J(J+1)}} \left[ \frac{\kappa_h + 1}{\kappa_h} \right]^{1/2} \left( \begin{array}{ccc} j_h & j_p & J \\ -\frac{1}{2} & -\frac{1}{2} & 1 \end{array} \right) \\ + \frac{(-1)^{j_h+l_h+1/2}}{\sqrt{J(J+1)}} \left[ \frac{\kappa_h - 1}{\kappa_h} \right]^{1/2} \left( \begin{array}{ccc} j_h & j_p & J \\ -\frac{3}{2} & \frac{1}{2} & 1 \end{array} \right) \\ \left. + (-1)^{j_p+j_h+J} \left[ \frac{(J-1)(J+2)}{J(J+1)} \frac{\kappa_h - 1}{\kappa_h} \right]^{1/2} \left( \begin{array}{ccc} j_h & j_p & J \\ -\frac{3}{2} & -\frac{1}{2} & 2 \end{array} \right) \right\} \quad (147)$$

$$\left\{ \begin{array}{ccc} \frac{1}{2} & l_p & j_p \\ \frac{1}{2} & l_h & j_h \\ 1 & J' & J \end{array} \right\} \left( \begin{array}{ccc} l_h & J' & l_p \\ 1 & -1 & 0 \end{array} \right) = \frac{1}{2\sqrt{3}[l_p][l_h][J][J']} \left\{ \left[ \frac{(J-s)(J-s+1)}{2J+s+1} \frac{\kappa_h + 1}{\kappa_h} \right]^{1/2} \left( \begin{array}{ccc} j_h & j_p & J \\ \frac{3}{2} & \frac{1}{2} & -2 \end{array} \right) \right.$$

$$\begin{aligned}
& + (-1)^{l_p+j_p-1/2} \frac{s}{2} \left[ \frac{(2J+3+s)(2J+s-1)\kappa_h-1}{2J+s+1} \frac{\kappa_h-1}{\kappa_h} \right]^{1/2} \begin{pmatrix} j_h & j_p & J \\ \frac{3}{2} & -\frac{1}{2} & -1 \end{pmatrix} \\
& + (-1)^{l_h+j_h-1/2} \frac{s}{2} \left[ \frac{(2J+3+s)(2J+s-1)\kappa_h+1}{2J+s+1} \frac{\kappa_h+1}{\kappa_h} \right]^{1/2} \begin{pmatrix} j_h & j_p & J \\ \frac{1}{2} & \frac{1}{2} & -1 \end{pmatrix} \\
& + (-1)^{j_p+j_h+J+1} \left[ \frac{(J+s)(J+s+1)\kappa_h+1}{2J+s+1} \frac{\kappa_h+1}{\kappa_h} \right]^{1/2} \begin{pmatrix} j_h & j_p & J \\ \frac{1}{2} & -\frac{1}{2} & 0 \end{pmatrix} \Bigg\}, \quad (148)
\end{aligned}$$

where as before  $\kappa_i = (-1)^{j_i+l_i+1/2}(j_i+1/2)$ .

## C Polarized responses for a hole nucleus in PWIA

In this appendix we give some of the details of the calculation of the polarized momentum distribution and inclusive responses for a hole nucleus in PWIA omitted from sect. 2.4. In order to compute the momentum distribution of the shell  $h$ ,

$$n(\mathbf{p})_{r'r} = \sum_{m_h m'_i} \langle B|a_{\mathbf{p}r}|A\rangle^* \langle B|a_{\mathbf{p}r'}|A\rangle, \quad (149)$$

we need to compute the matrix element of the annihilation operator  $a_{\mathbf{p}r}$  between the initial and the residual nuclear states (see eqs. (59,60)):

$$\langle B|a_{\mathbf{p}r}|A\rangle = \sum_{m_i} \langle C|b_{im'_i} b_{hm_h} a_{\mathbf{p}r} b_{im_i}^\dagger |C\rangle \mathcal{D}_{m_i}^{(i)}(\Omega^*). \quad (150)$$

To accomplish this, we expand the destruction operator in the plane-wave basis in terms of the shell model basis,

$$a_{\mathbf{p}r} = \sum_{l < F} \langle \mathbf{p}, r | \tilde{l} \rangle b_l^\dagger + \sum_{\alpha > F} \langle \mathbf{p}, r | \alpha \rangle a_\alpha, \quad (151)$$

where  $|\tilde{l}\rangle = |j_l \widetilde{m}_l\rangle = (-1)^{j_l+m_l} |j_l - m_l\rangle$  is the time inversion of the single-particle state  $|l\rangle$ . Using the commutation relations between particle and hole operators, we obtain for the matrix element

$$\langle B|a_{\mathbf{p}r}|A\rangle = \mathcal{D}_{m'_i}^{(i)} \langle \mathbf{p}r | \widetilde{h m_h} \rangle - \delta_{hi} \mathcal{D}_{m_h}^{(i)} \langle \mathbf{p}r | \widetilde{i m'_i} \rangle. \quad (152)$$

In the case  $h \neq i$  we have

$$\langle B|a_{\mathbf{p}r}|A\rangle = \mathcal{D}_{m'_i i}^{(i)} \langle \mathbf{p}r | \widetilde{h m_h} \rangle, \quad (153)$$

and thus we sum over third components  $m_h$  and use  $\sum_{m'_i} |\mathcal{D}_{m'_i i}^{(i)}|^2 = 1$  to obtain the momentum distribution of the complete shell  $h$ :

$$n(\mathbf{p})_{r'r} = n_{r'r}^{(h)}(\mathbf{p})_{\text{unpol}} = \sum_{m_h} \langle \mathbf{p}r' | h m_h \rangle \langle h m_h | \mathbf{p}r' \rangle. \quad (154)$$

In the case  $h = i$ ,  $m_h = m'_i$  and we have

$$\langle B|a_{\mathbf{p}r}|A\rangle = \mathcal{D}_{m'_i i}^{(i)} \langle \mathbf{p}r | \widetilde{i m'_i} \rangle - \mathcal{D}_{m''_i i}^{(i)} \langle \mathbf{p}r | \widetilde{i m''_i} \rangle \quad (155)$$

An important aspect here is that in the sum over  $m'_i$ ,  $m''_i$  we must divide by a factor two to avoid double-counting in the antisymmetrized states,  $|B\rangle = |i^{-1}m''_i, i^{-1}m'_i\rangle$ .

Taking this fact into account we obtain for the momentum distribution

$$\begin{aligned} n(\mathbf{p})_{r'r} &= \sum_{m_i} \langle \mathbf{p}r' | i m_i \rangle \langle i m_i | \mathbf{p}r \rangle - \sum_{m'_i m''_i} \mathcal{D}_{m'_i i}^{(i)*} \mathcal{D}_{m''_i i}^{(i)} \langle \mathbf{p}r' | \widetilde{i m'_i} \rangle \langle \widetilde{i m''_i} | \mathbf{p}r \rangle \\ &= n_{r'r}^{(i)}(\mathbf{p})_{\text{unpol}} - n_{r'r}^{(i)}(\mathbf{p}, \Omega^*)_{\text{hole}}, \end{aligned} \quad (156)$$

that is, the (unpolarized) momentum distribution of the complete shell  $i$  minus the (polarized) momentum distribution of the hole,

$$n_{r'r}^{(i)}(\mathbf{p}, \Omega^*)_{\text{hole}} = \sum_{m'_i m''_i} \mathcal{D}_{m'_i i}^{(i)*} \mathcal{D}_{m''_i i}^{(i)} \langle \mathbf{p}r' | \widetilde{i m'_i} \rangle \langle \widetilde{i m''_i} | \mathbf{p}r \rangle. \quad (157)$$

For the computation of the unpolarized and polarized momentum distribution we must substitute the matrix element

$$\langle \mathbf{p}r | j m \rangle = i^{-l} \sum_M Y_{lM}(\hat{\mathbf{p}}) \langle \frac{1}{2} r l M | j m \rangle \tilde{R}(p) \quad (158)$$

and perform the sums over third components using Racah algebra.

These basic PWIA developments can be found for example in ref. [13] where a general expression is given and thus we do not repeat the details here, but only quote



the result for the particular model of present interest. The polarized momentum distribution of a hole with quantum numbers  $l, j$  can be written

$$n_{rr'}^{(j)}(\mathbf{p}, \Omega^*)_{\text{hole}} = [l]^2 [j]^2 \tilde{R}(p)^2 \sum_{SM} [S] (-1)^{r'-1/2} \begin{pmatrix} \frac{1}{2} & \frac{1}{2} & S \\ r & -r' & M \end{pmatrix} \\ \times \sum_{\mathcal{J}\mathcal{J}'} (-1)^{l+\mathcal{J}} f_{\mathcal{J}}^{(j)}[\mathcal{J}'] \begin{Bmatrix} \frac{1}{2} & \frac{1}{2} & S \\ l & l & \mathcal{J}' \\ j & j & \mathcal{J} \end{Bmatrix} \begin{pmatrix} \mathcal{J}' & l & l \\ 0 & 0 & 0 \end{pmatrix} [Y_{\mathcal{J}}(\Omega^*) Y_{\mathcal{J}'}(\hat{\mathbf{p}})]_{SM}, \quad (159)$$

where the coupling of two spherical harmonics with different angles is defined by

$$[Y_{\mathcal{J}}(\Omega^*) Y_{\mathcal{J}'}(\hat{\mathbf{p}})]_{SM} \equiv \sum_{\mathcal{M}\mathcal{M}'} \langle \mathcal{J}\mathcal{M}\mathcal{J}'\mathcal{M}' | SM \rangle Y_{\mathcal{J}\mathcal{M}}(\Omega^*) Y_{\mathcal{J}'\mathcal{M}'}(\hat{\mathbf{p}}). \quad (160)$$

First, note that in this equation we have  $S = 0, 1$ , and hence may write  $n_{rr'}$  as the sum of scalar ( $S = 0$ ) plus vector ( $S = 1$ ) terms,  $n = n^S + n^V$ . Obviously  $n^S$  and  $n^V$  are related to the scalar and vector momentum distributions introduced in sect. 2.4 by

$$n_{rr'}^S = \frac{1}{2} \delta_{rr'} M^S \quad (161)$$

$$n_{rr'}^V = \frac{1}{2} \langle r | \mathbf{M}^V \cdot \boldsymbol{\sigma} | r' \rangle. \quad (162)$$

Second we note from the second 3- $j$  that  $\mathcal{J}' = \text{even}$  and as a consequence it is easily seen by permutation of the first two columns of the 9- $j$  that the result is zero unless  $S + \mathcal{J} = \text{even}$ .

For  $S = 0$  we have  $\mathcal{J} = \mathcal{J}' = \text{even}$ . In this case we can use eqs. (3.7.9) and (6.4.14) in ref. [11] together with the following relation

$$\begin{Bmatrix} l & l & \mathcal{J} \\ j & j & \frac{1}{2} \end{Bmatrix} \begin{pmatrix} \mathcal{J} & l & l \\ 0 & 0 & 0 \end{pmatrix} = -P_{\mathcal{J}}^+ \frac{1}{[l]^2} \begin{pmatrix} j & j & \mathcal{J} \\ \frac{1}{2} & -\frac{1}{2} & 0 \end{pmatrix} \quad (163)$$

to obtain

$$n_{rr'}^S = \delta_{rr'} [j]^2 \tilde{R}(p)^2 \sum_{\mathcal{J}} P_{\mathcal{J}}^+ f_{\mathcal{J}}^{(j)} \frac{(-1)^{j-1/2}}{2} \begin{pmatrix} j & j & \mathcal{J} \\ \frac{1}{2} & -\frac{1}{2} & 0 \end{pmatrix} [Y_{\mathcal{J}}(\Omega^*) Y_{\mathcal{J}}(\hat{\mathbf{p}})]_0, \quad (164)$$

from which we immediately arrive at eq. (66). In the  $S = 1$  case we have  $\mathcal{J} = \text{odd}$  and  $\mathcal{J}' = \mathcal{J} \pm 1$ . We use the following expression for the product of the 9- $j$  with the 3- $j$

$$\left\{ \begin{array}{ccc} \frac{1}{2} & \frac{1}{2} & 1 \\ l & l & \mathcal{J}' \\ j & j & \mathcal{J} \end{array} \right\} \left( \begin{array}{ccc} \mathcal{J}' & l & l \\ 0 & 0 & 0 \end{array} \right) = P_{\mathcal{J}}^{-} \frac{(-1)^{j+l+1/2}}{\sqrt{6[l]^2[\mathcal{J}][\mathcal{J}']}} \frac{2\kappa + s\mathcal{J} + \delta_{s1}}{\sqrt{\mathcal{J} + \delta_{s1}}} \left( \begin{array}{ccc} j & j & \mathcal{J} \\ \frac{1}{2} & -\frac{1}{2} & 0 \end{array} \right) \quad (165)$$

to obtain for the vector part of the momentum distribution

$$n_{rr'}^V = \sqrt{2}(-1)^{r'-1/2} \sum_{\mu} \left( \begin{array}{ccc} \frac{1}{2} & \frac{1}{2} & 1 \\ r & -r' & \mu \end{array} \right) \times \sum_{\mathcal{J}} \sum_{\mathcal{J}'=\mathcal{J}\pm 1} P_{\mathcal{J}}^{-} f_{\mathcal{J}}^j [j]^2 |\tilde{R}(p)|^2 A_{\mathcal{J}\mathcal{J}'} [Y_{\mathcal{J}}(\Omega^*) Y_{\mathcal{J}'}(\hat{\mathbf{p}})]_{1\mu}, \quad (166)$$

where we have used the definitions eqs. (68–70). From this result it is straightforward to obtain eq. (67) for the vector momentum distribution.

To obtain the inclusive responses for a one-hole nucleus in PWIA we begin with the general expressions in eqs. (86,87), using the single-nucleon responses given in eqs. (78-83) and the scalar and vector momentum distributions given in eqs. (66,67). The integral over  $\phi$  in (86,87) can be performed analytically in all cases. First we define the functions  $y_{lm}(\theta)$  through  $Y_{lm}(\theta, \phi) \equiv y_{lm}(\theta)e^{im\phi}$ . The integrals that we need for the computation of the unprimed responses are the following:

$$\int_0^{2\pi} d\phi [Y_{\mathcal{J}}(\Omega^*) Y_{\mathcal{J}}(\hat{\mathbf{p}})]_0 \cos \mathcal{M}\phi = \frac{2\pi}{[\mathcal{J}]} y_{\mathcal{J}\mathcal{M}}(\theta^*) y_{\mathcal{J}\mathcal{M}}(\theta) \cos \mathcal{M}\phi^*, \quad (167)$$

with  $\mathcal{M} = 0, 1, 2$ . The single-nucleon  $L$  and  $T$  responses are independent of  $\phi$  and so we have  $\mathcal{M} = 0$ :

$$R^L = \frac{4\pi M}{q} \sum_{\mathcal{J}} P_{\mathcal{J}}^+ f_{\mathcal{J}}^i A_{\mathcal{J}} \frac{[j_i]^2}{[\mathcal{J}]} y_{\mathcal{J}0}(\theta^*) \int_{|p'-q|}^{p'+q} dp p (\rho_c^2 + \rho_{so}^2 \delta^2) |\tilde{R}_i(p)|^2 y_{\mathcal{J}0}(\theta) \quad (168)$$

$$R^T = \frac{4\pi M}{q} \sum_{\mathcal{J}} P_{\mathcal{J}}^+ f_{\mathcal{J}}^i A_{\mathcal{J}} \frac{[j_i]^2}{[\mathcal{J}]} y_{\mathcal{J}0}(\theta^*) \int_{|p'-q|}^{p'+q} dp p (2J_m^2 + J_c^2 \delta^2) |\tilde{R}_i(p)|^2 y_{\mathcal{J}0}(\theta). \quad (169)$$

Next, the single-nucleon  $TL$  response is proportional to  $\cos \phi$  and so we have  $\mathcal{M} = 1$ :

$$R^{TL} = 4\pi \frac{M}{q} \sum_{\mathcal{J}} P_{\mathcal{J}}^+ f_{\mathcal{J}}^i A_{\mathcal{J}} \frac{[j_i]^2}{[\mathcal{J}]} y_{\mathcal{J}1}(\theta^*) \cos \phi^* \times \int_{|p'-q|}^{p'+q} dp p 2\sqrt{2} (\rho_c J_c + \rho_{so} J_m) \delta |\tilde{R}_i(p)|^2 y_{\mathcal{J}1}(\theta). \quad (170)$$

Finally, the single-nucleon  $TT$  response is proportional to  $\cos 2\phi$  and so we have the integral for  $\mathcal{M} = 2$ :

$$R^{TT} = -4\pi \frac{M}{q} \sum_{\mathcal{J}} P_{\mathcal{J}}^+ f_{\mathcal{J}}^i A_{\mathcal{J}} \frac{[j_i]^2}{[\mathcal{J}]} y_{\mathcal{J}2}(\theta^*) \cos 2\phi^* \int_{|p'-q|}^{p'+q} dp p J_c^2 \delta^2 |\tilde{R}_i(p)|^2 y_{\mathcal{J}2}(\theta). \quad (171)$$

For the primed responses we first define a real vector  $\mathbf{X}^{\mathcal{J}\mathcal{J}'}(\Omega^*, \hat{\mathbf{p}})$  by its spherical components

$$X_{\alpha}^{\mathcal{J}\mathcal{J}'}(\Omega^*, \hat{\mathbf{p}}) \equiv [Y_{\mathcal{J}}(\Omega^*) Y_{\mathcal{J}'}(\hat{\mathbf{p}})]_{1\alpha} \quad (172)$$

and then we can write the vector momentum distribution in eq. (67) as a linear combination of the vectors  $\mathbf{X}^{\mathcal{J}\mathcal{J}'}$ :

$$\mathbf{M}^V = \frac{2}{\sqrt{3}} \sum_{\mathcal{J}} \sum_{\mathcal{J}'=\mathcal{J}\pm 1} P_{\mathcal{J}}^- f_{\mathcal{J}}^i A_{\mathcal{J}\mathcal{J}'} [j_i]^2 |\tilde{R}_i(p)|^2 \mathbf{X}^{\mathcal{J}\mathcal{J}'}. \quad (173)$$

It is straightforward to compute the scalar products between the vector momentum distribution  $\mathbf{M}^V$  and the vector single-nucleon response  $\mathbf{w}_V^K$ . To obtain the azimuthal integrals we need the following results for integrals of components of  $\mathbf{X}$ :

$$\int_0^{2\pi} d\phi X_1 = -2\pi\sqrt{2} \langle \mathcal{J}1\mathcal{J}'0|11 \rangle y_{\mathcal{J}1}(\theta^*) y_{\mathcal{J}'0}(\theta) \cos \phi^* \quad (174)$$

$$\int_0^{2\pi} d\phi \sin \phi (\cos \phi X_2 - \sin \phi X_1) = \pi\sqrt{2} y_{\mathcal{J}1}(\theta^*) \cos \phi^* \times [\langle \mathcal{J} - 1\mathcal{J}'2|11 \rangle y_{\mathcal{J}'2}(\theta) + \langle \mathcal{J}1\mathcal{J}'0|11 \rangle y_{\mathcal{J}'0}(\theta)] \quad (175)$$

$$\int_0^{2\pi} d\phi \cos \phi X_3 = -2\pi y_{\mathcal{J}1}(\theta^*) \cos \phi^* \langle \mathcal{J}1\mathcal{J}' - 1|10 \rangle y_{\mathcal{J}'1}(\theta), \quad (176)$$

from which we obtain

$$R^{TL} = 4\pi \frac{M}{q} \sum_{\mathcal{J}} \sum_{\mathcal{J}'\pm 1} P_{\mathcal{J}}^- f_{\mathcal{J}}^i A_{\mathcal{J}\mathcal{J}'} [j_i]^2 \sqrt{\frac{2}{3}} y_{\mathcal{J}1}(\theta^*) \cos \phi^* \int_{|p'-q|}^{p'+q} dp p |\tilde{R}_i(p)|^2 \times \left\{ -2\sqrt{2} \langle \mathcal{J}1\mathcal{J}'0|11 \rangle y_{\mathcal{J}'0}(\theta) \rho_c J_m + \sqrt{2} [\langle \mathcal{J} - 1\mathcal{J}'2|11 \rangle y_{\mathcal{J}'2}(\theta) + \langle \mathcal{J}1\mathcal{J}'0|11 \rangle y_{\mathcal{J}'0}(\theta)] \rho_{so} J_c \delta^2 + 2 \langle \mathcal{J}1\mathcal{J}' - 1|10 \rangle y_{\mathcal{J}'1}(\theta) \rho_{so} J_m \delta \right\}. \quad (177)$$

For the response  $T'$  we need the following integrals:

$$\int_0^{2\pi} d\phi (\cos \phi X_1 + \sin \phi X_2) = -2\pi\sqrt{2}\langle \mathcal{J}0\mathcal{J}'1|11\rangle y_{\mathcal{J}0}(\theta^*) y_{\mathcal{J}'1}(\theta) \quad (178)$$

$$\int_0^{2\pi} d\phi X_3 = 2\pi\langle \mathcal{J}0\mathcal{J}'0|10\rangle y_{\mathcal{J}0}(\theta^*) y_{\mathcal{J}'0}(\theta), \quad (179)$$

from which we have

$$\begin{aligned} R^{T'} &= -4\pi \frac{M}{q} \sum_{\mathcal{J}} \sum_{\mathcal{J}'\pm 1} P_{\mathcal{J}}^- f_{\mathcal{J}}^i A_{\mathcal{J}\mathcal{J}'} [j_i]^2 \frac{2}{\sqrt{3}} y_{\mathcal{J}0}(\theta^*) \int_{|p'-q|}^{p'+q} dp p |\tilde{R}_i(p)|^2 \\ &\times \left\{ \sqrt{2}\langle \mathcal{J}0\mathcal{J}'1|11\rangle y_{\mathcal{J}'1}(\theta) J_m J_c \delta + \langle \mathcal{J}0\mathcal{J}'0|10\rangle y_{\mathcal{J}'0}(\theta) J_m^2 \right\}. \end{aligned} \quad (180)$$

Finally, using

$$y_{lm}(\theta) = \frac{[l]}{\sqrt{4\pi}} (-1)^m \left[ \frac{(l-m)!}{(l+m)!} \right]^{1/2} P_l^m(\cos \theta), \quad (181)$$

one arrives at eqs. (90-97) for the polarized reduced responses in PWIA.

## References

- [1] T.W. Donnelly and A.S. Raskin, Ann. Phys. (NY), **169** (1986) 247.
- [2] A.S. Raskin and T.W. Donnelly, Ann. Phys. (NY) **191** (1989) 78.
- [3] S. Boffi, C. Giusti and F.D. Pacati, Phys. Rep. 226 (1993) 1.
- [4] S. Boffi, C. Giusti and F.D. Pacati, Nucl. Phys **A476** (1988) 617.
- [5] J.A. Caballero, T.W. Donnelly and G.I. Poulis, Nucl. Phys. **A555** (1993) 709.
- [6] E. Garrido, J.A. Caballero, E. Moya de Guerra, P.Sarriguren and J.M. Udías, Nucl. Phys. **A584** (1995) 256.
- [7] H. Gao, *et al.*, Phys. Rev. **C50** (1994) R546.
- [8] J.-O. Hansen, *et al.*, Phys. Rev. Lett. **74** (1995) 654.

- [9] J.E. Amaro, G. Co', E. Fasanelli and A.M. Lallena, Phys. Lett. **B277** (1992) 365; J.E. Amaro, G. Co', and A.M. Lallena, Ann. Phys. **221** (1993) 306; J.E. Amaro, G. Co', and A.M. Lallena, Nucl. Phys. **A578** (1994) 365; J.E. Amaro, A.M. Lallena, and G. Co', Int. J. Mod. Phys. **E3** (1994) 735.
- [10] J.E. Amaro, J.A. Caballero, T.W. Donnelly, A.M. Lallena, E. Moya de Guerra and J.M. Udías, Nucl. Phys. **A602** (1996) 263.
- [11] A.R. Edmonds, *Angular Momentum in Quantum Mechanics*, Third Printing (Princeton University Press, 1974).
- [12] W.M. Alberico, T.W. Donnelly and A. Molinari, Nucl. Phys. **A512** (1990) 541.
- [13] J.A. Caballero, T.W. Donnelly, G.I. Poulis, E. Garrido and E. Moya de Guerra, Nucl. Phys. **A577** (1994) 528.
- [14] T. de Forest, Nucl. Phys. **A392** (1983) 232.
- [15] S. Galster, *et al.*, Nucl. Phys. **B32** (1971) 221.
- [16] T.W. Donnelly and I. Sick, Rev. Mod. Phys. **56** (1984) 461.
- [17] R. Cenni, T.W. Donnelly and A. Molinari, preprint MIT/CTP #2523, June 1996.
- [18] J. E. Amaro, C. García-Recio and A. M. Lallena, Nucl. Phys. **A567** (1994) 701; S. Moraghe, J. E. Amaro, C. García-Recio and A. M. Lallena, Nucl. Phys. **A576** (1994) 553.
- [19] S. Boffi, C. Giusti, F.D. Pacati and M. Radici, Nucl. Phys. **A518** (1990) 639; S. Boffi and M. Radici, Nucl. Phys. **A526** (1991) 602; S. Boffi, M. Radici, J.J. Kelly and T.M. Payerle, Nucl. Phys. **A539** (1992) 597.

# Figure captions

1. Reduced responses at  $q = 500$  MeV/c for a polarized proton in the  $1s_{1/2}$  shell of a mean field potential. Solid lines: computed with the CSM; Dashed lines: PWIA (on-shell).
2. As in fig. 1, but now for a proton in the  $1p_{1/2}$  or  $2s_{1/2}$  shell.
3. Even-rank polarized reduced responses at  $q = 500$  MeV/c for a proton in the  $1p_{3/2}$  shell of a mean field. The meaning of the curves is the same as in fig. 1.
4. The same as fig. 3, but for the odd-rank responses.
5. Even-rank reduced responses for  $^{39}\text{K}$  at  $q = 500$  MeV/c. The meaning of the curves is the same as in fig. 1.
6. The same as fig. 5, but for the odd-rank responses.
7. As in fig. 5, but for  $q = 300$  MeV/c.
8. As in fig. 6, but for  $q = 300$  MeV/c.
9. As in fig. 5, but for  $q = 700$  MeV/c.
10. As in fig. 6, but for  $q = 700$  MeV/c.
11. Even-rank reduced responses for  $^{39}\text{K}$  at  $q = 500$  MeV/c. Solid lines: CSM; Dashed lines: PWIA (on-shell); Dot-dashed lines: PWIA (CC1).
12. Even-rank reduced responses for  $^{39}\text{K}$  at  $q = 500$  MeV/c in the CSM. Solid lines: total responses; Dashed lines: responses including only charge and magnetization terms; Dot-dashed lines: responses including charge, magnetization and convection terms.
13. The same as fig. 12, but for the odd-rank responses.

14. Response  $W_2^{TL}$  for  $^{39}\text{K}$  for different values of the momentum transfer. The meaning of the curves is the same as in fig. 12.

$1s_{1/2}$  proton,  $q = 500$  MeV/c

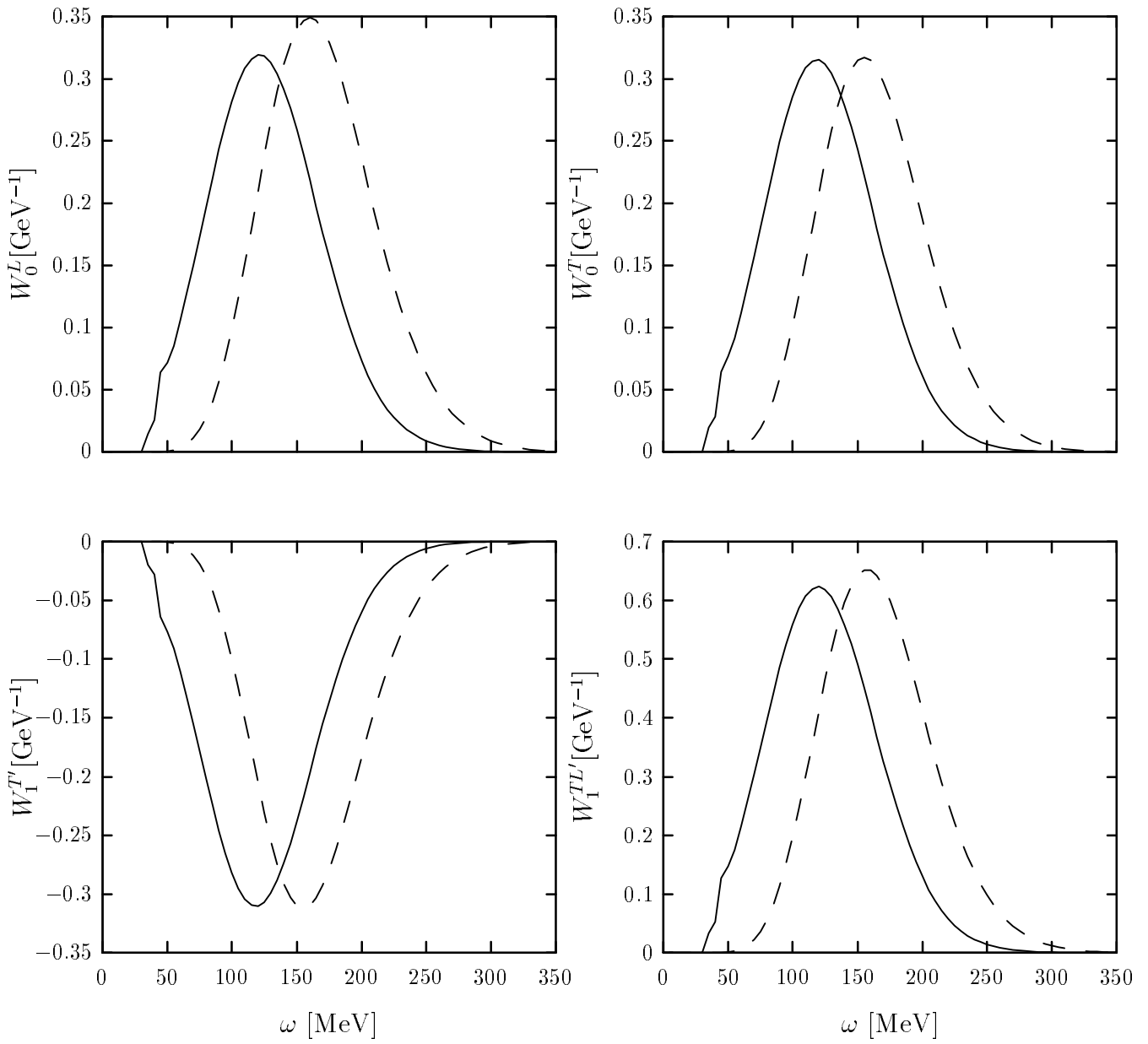


Figure 1



$q = 500 \text{ MeV}/c$

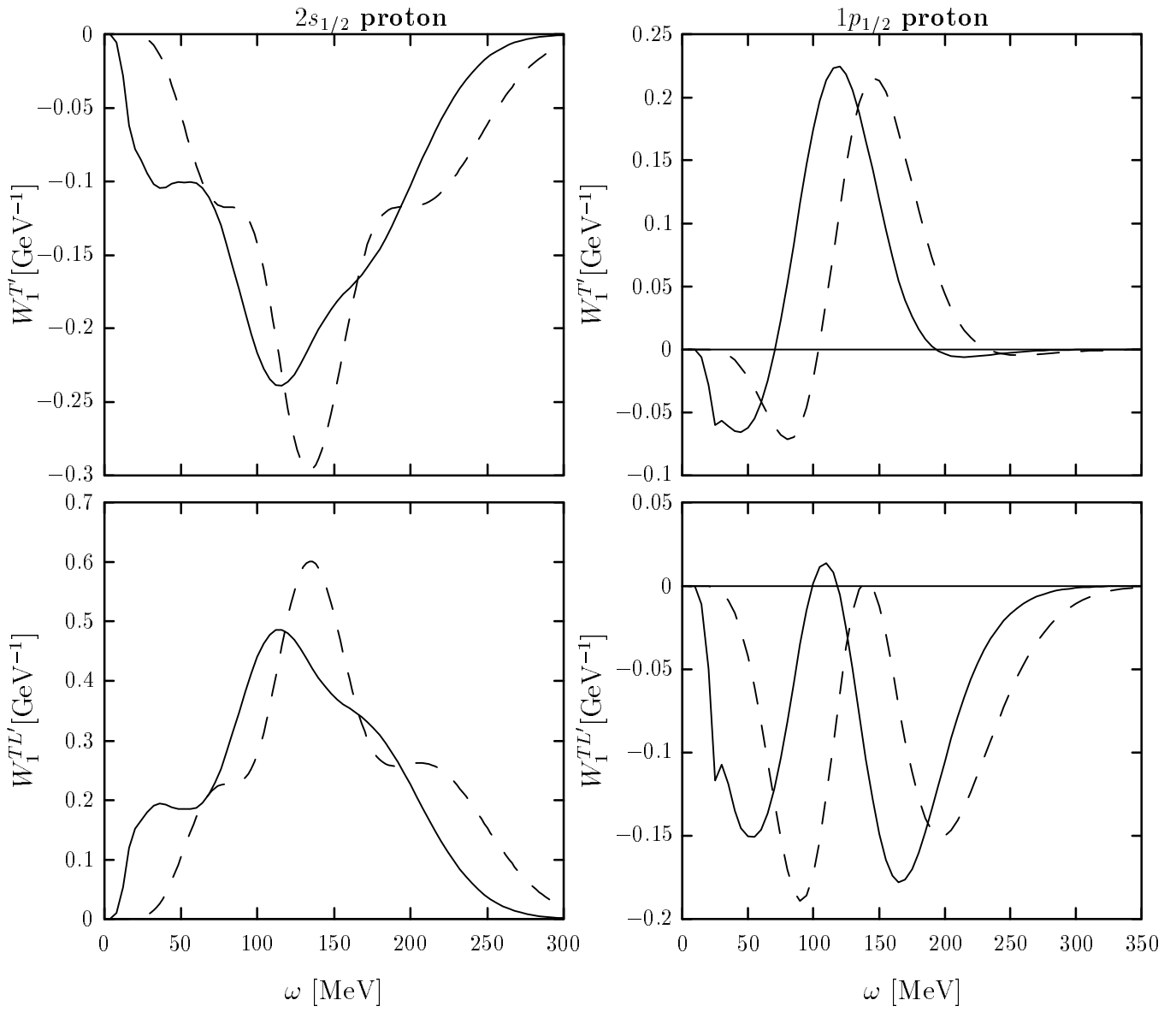


Figure 2

$1p_{3/2}$  proton,  $q = 500$  MeV/c

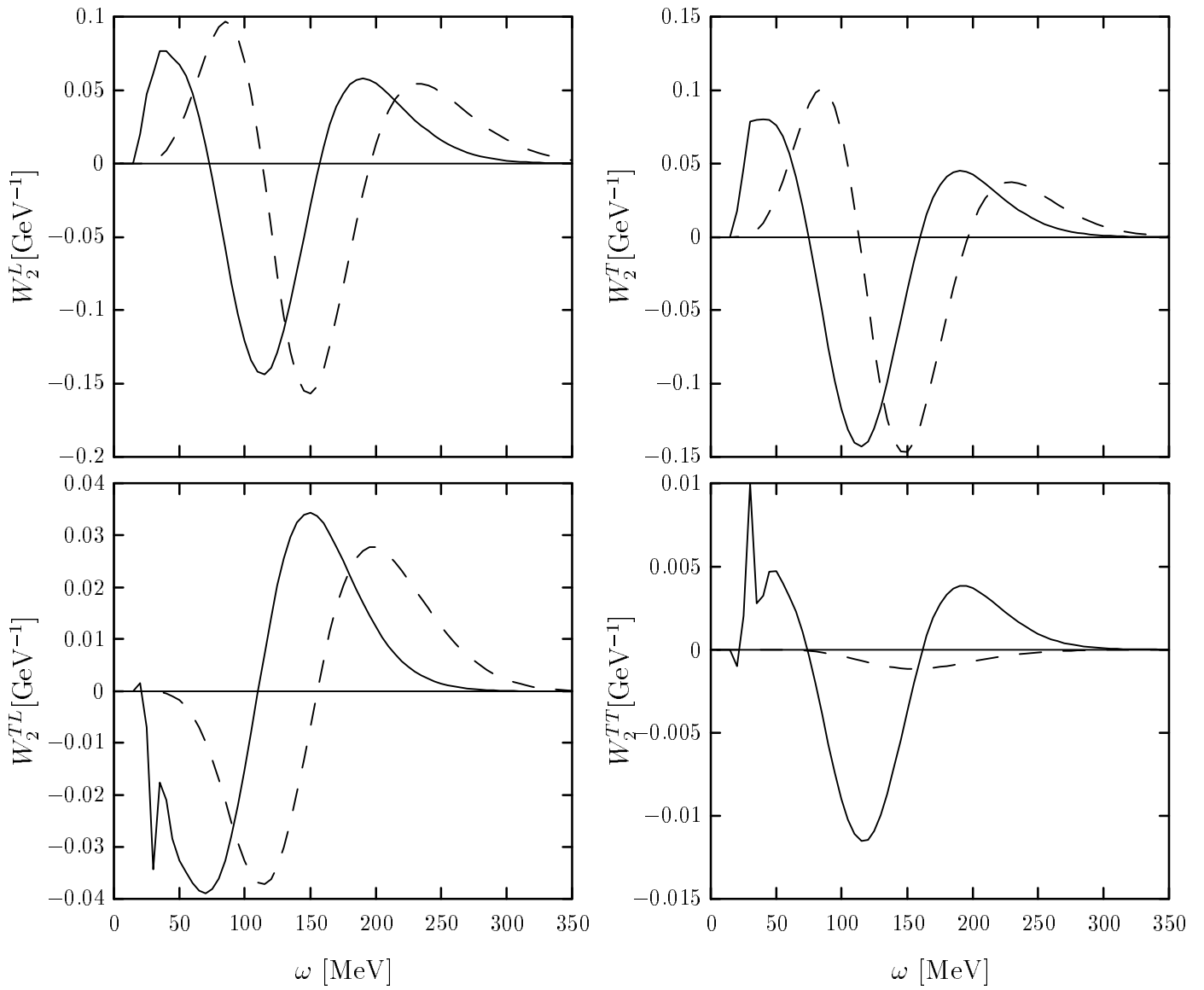


Figure 3

$1p_{3/2}$  proton,  $q = 500$  MeV/c

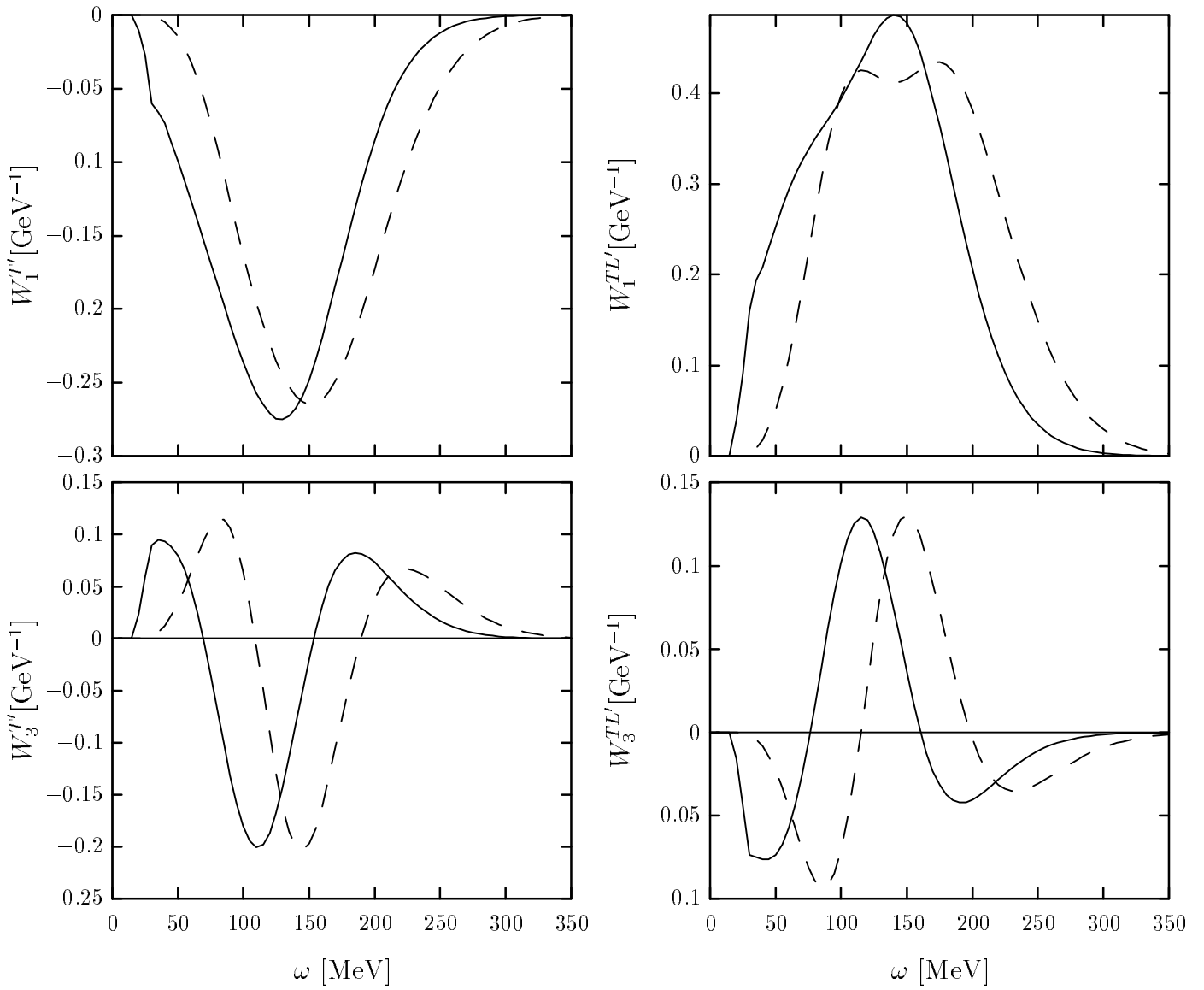


Figure 4

$^{39}\text{K}$ ,  $q = 500\text{MeV}/c$

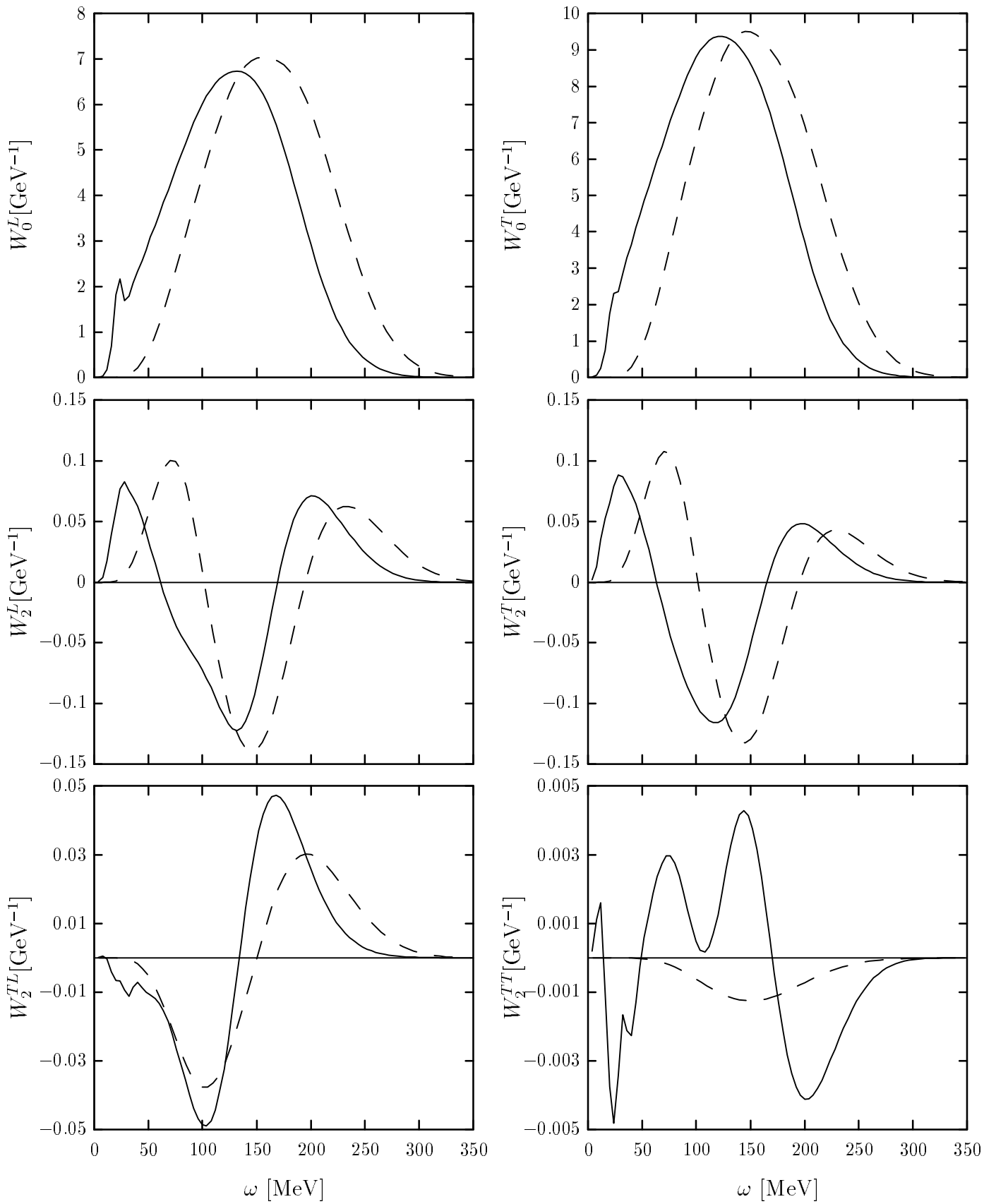


Figure 5

$^{39}\text{K}$ ,  $q = 500\text{MeV}/c$

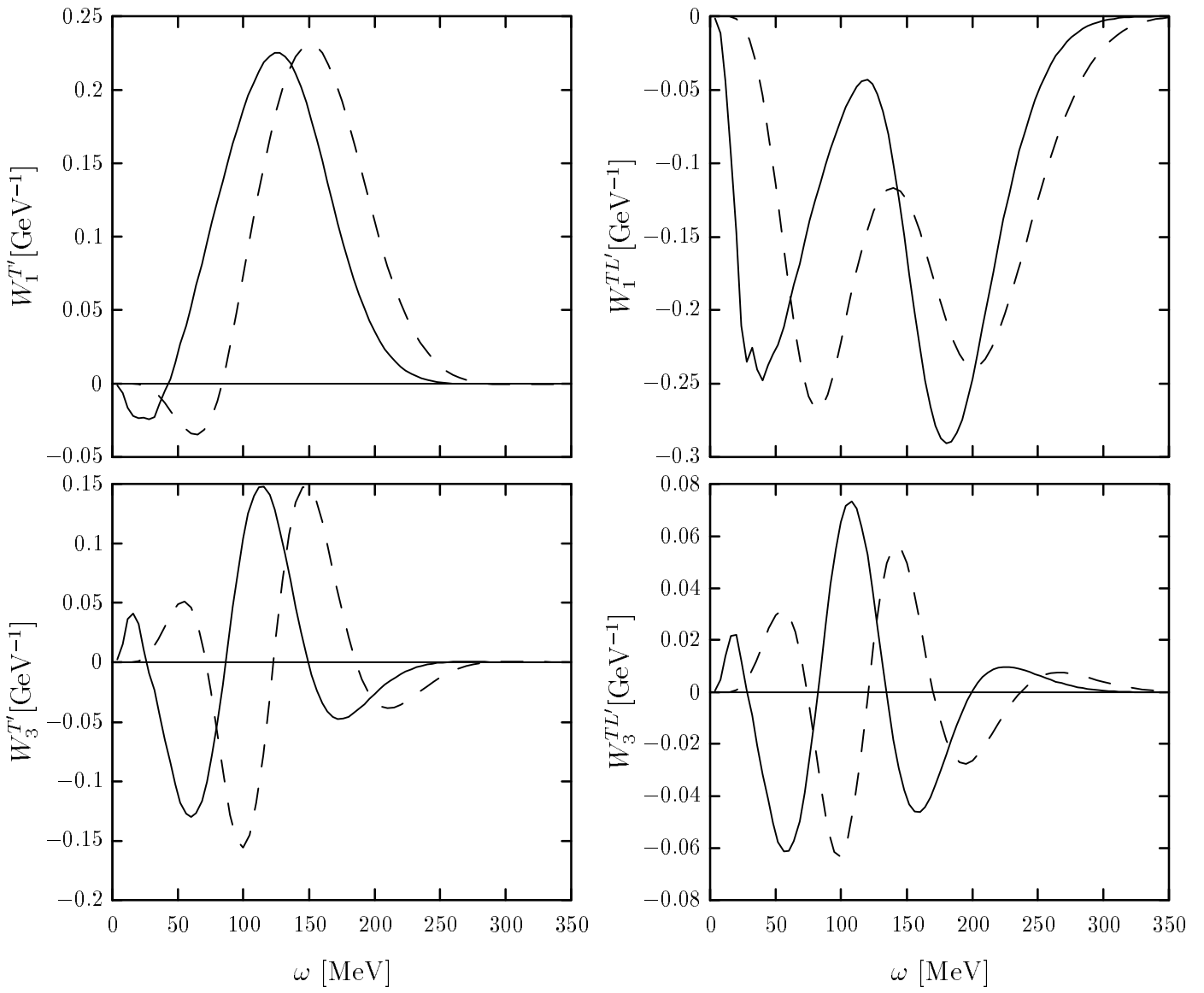


Figure 6

$^{39}\text{K}$ ,  $q = 300 \text{ MeV}/c$

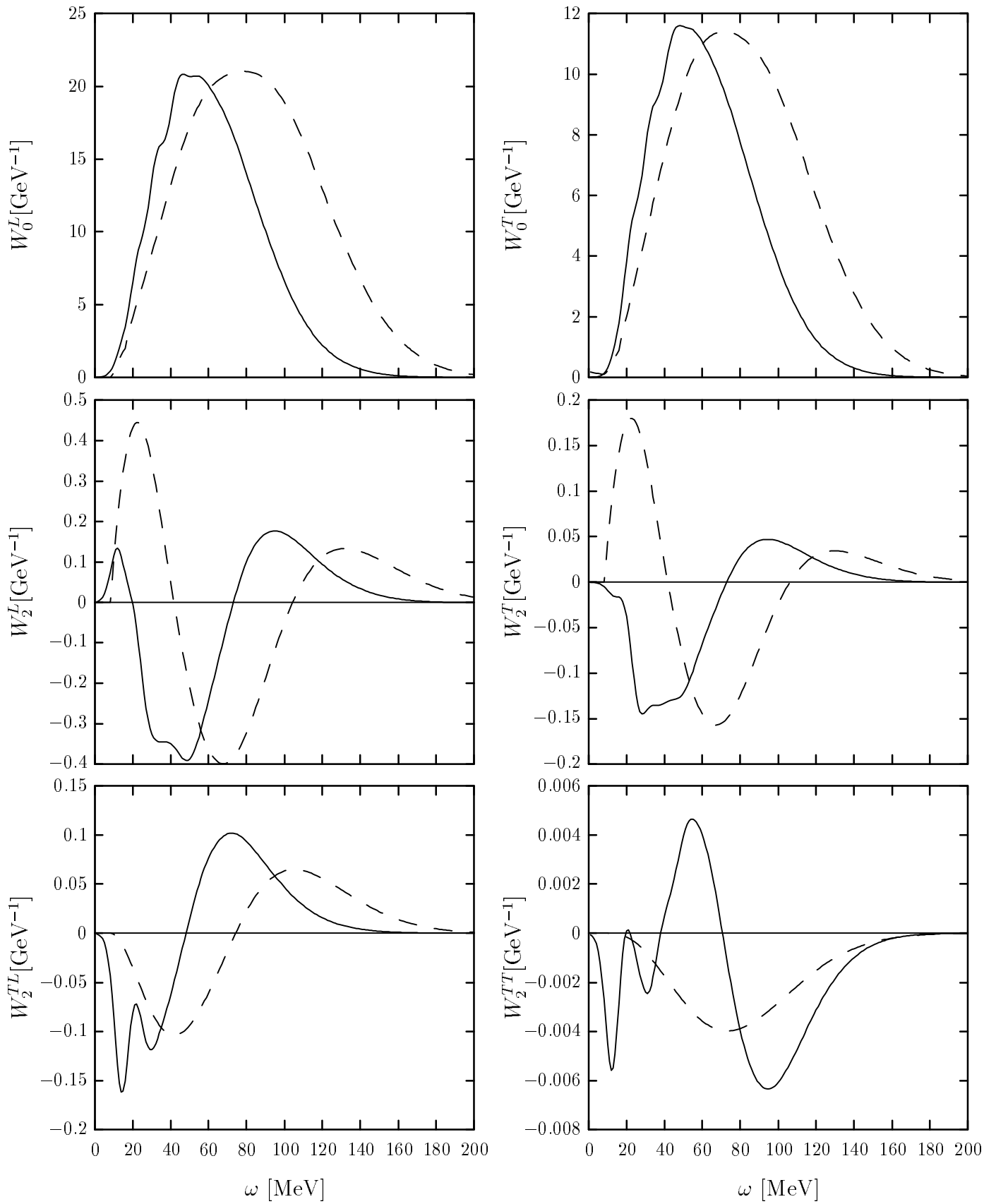


Figure 7

$^{39}\text{K}$ ,  $q = 300 \text{ MeV}/c$

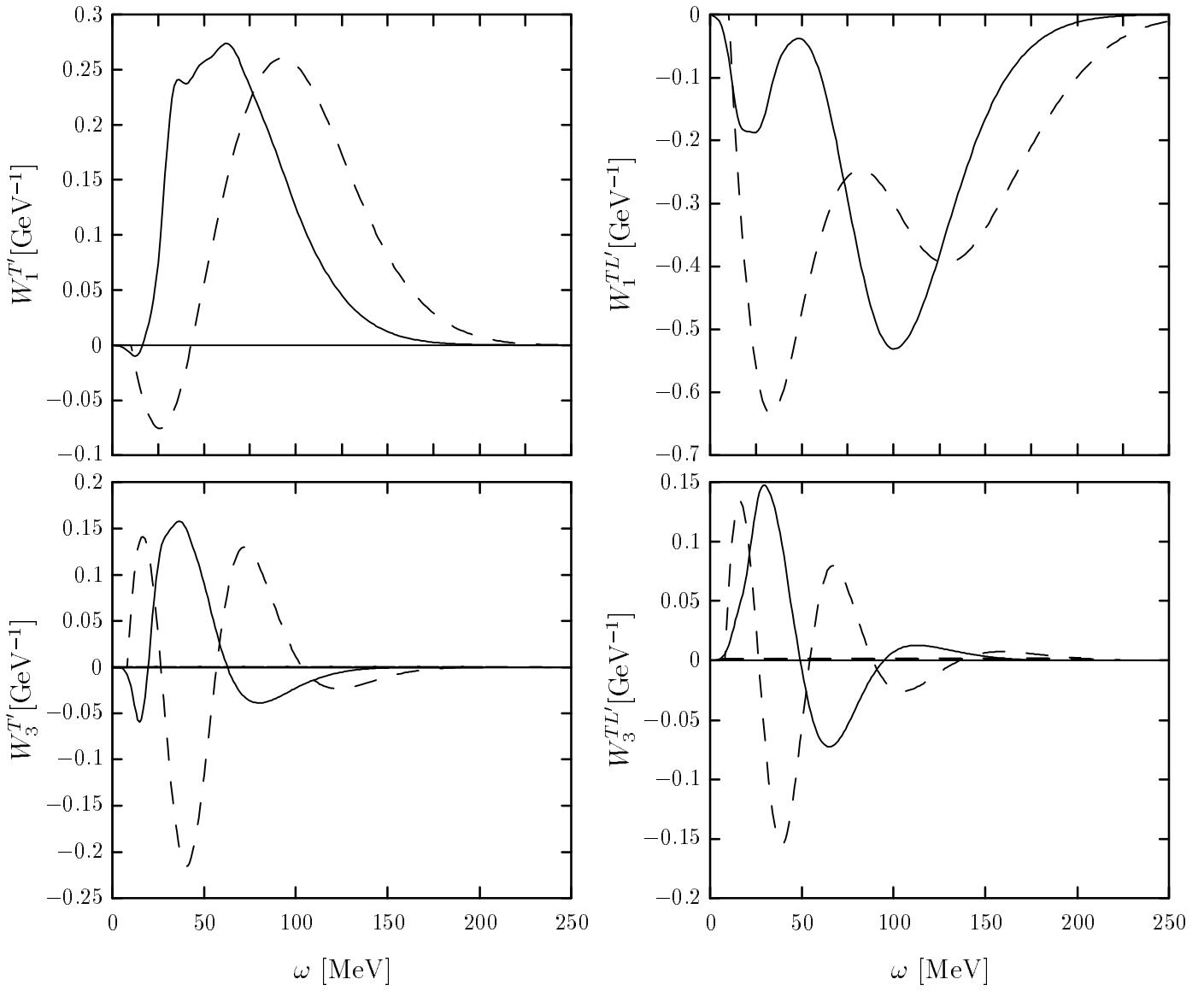


Figure 8

$^{39}\text{K}, q = 700 \text{ MeV}/c$

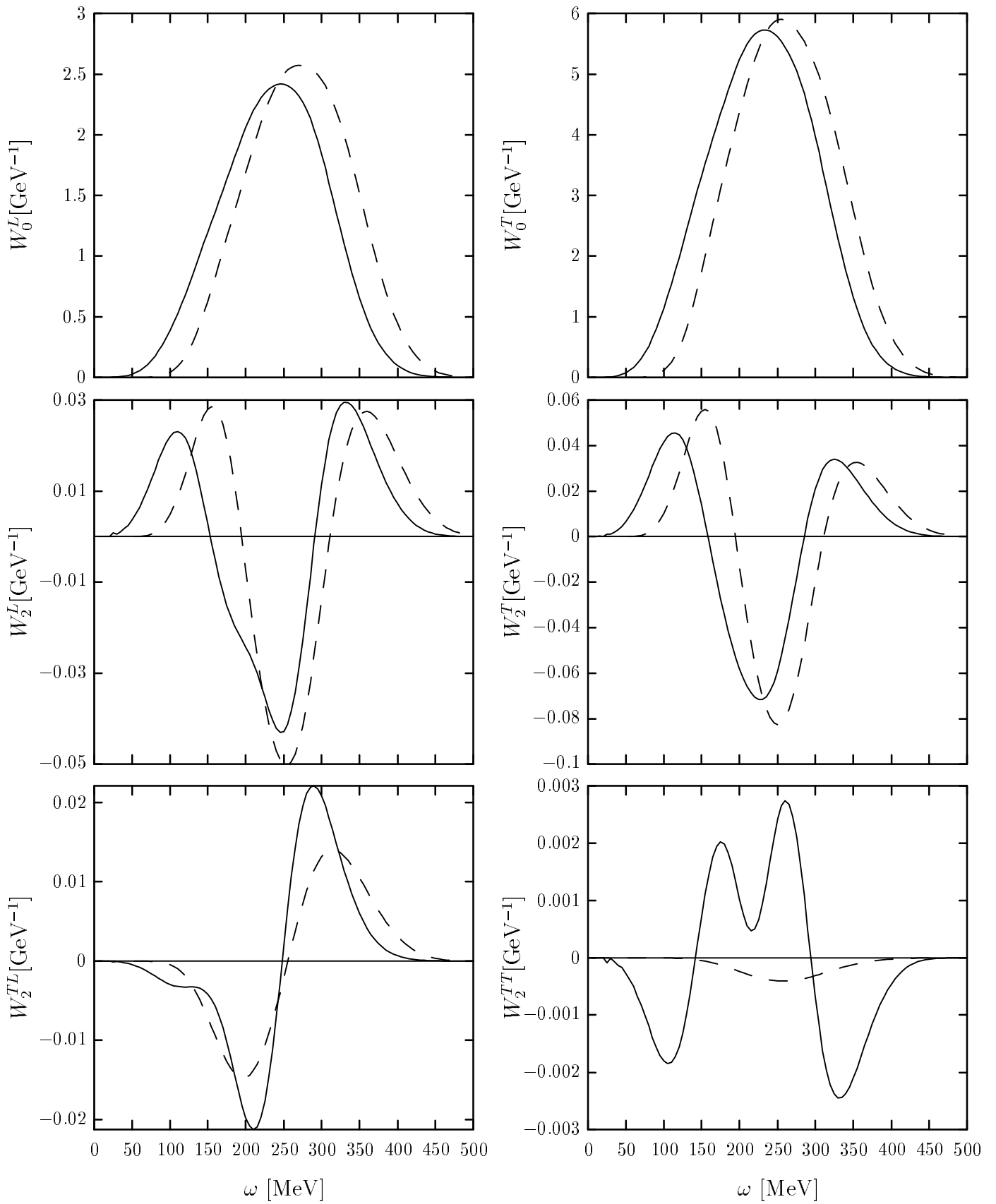


Figure 9



$^{39}\text{K}$ ,  $q = 700 \text{ MeV}/c$

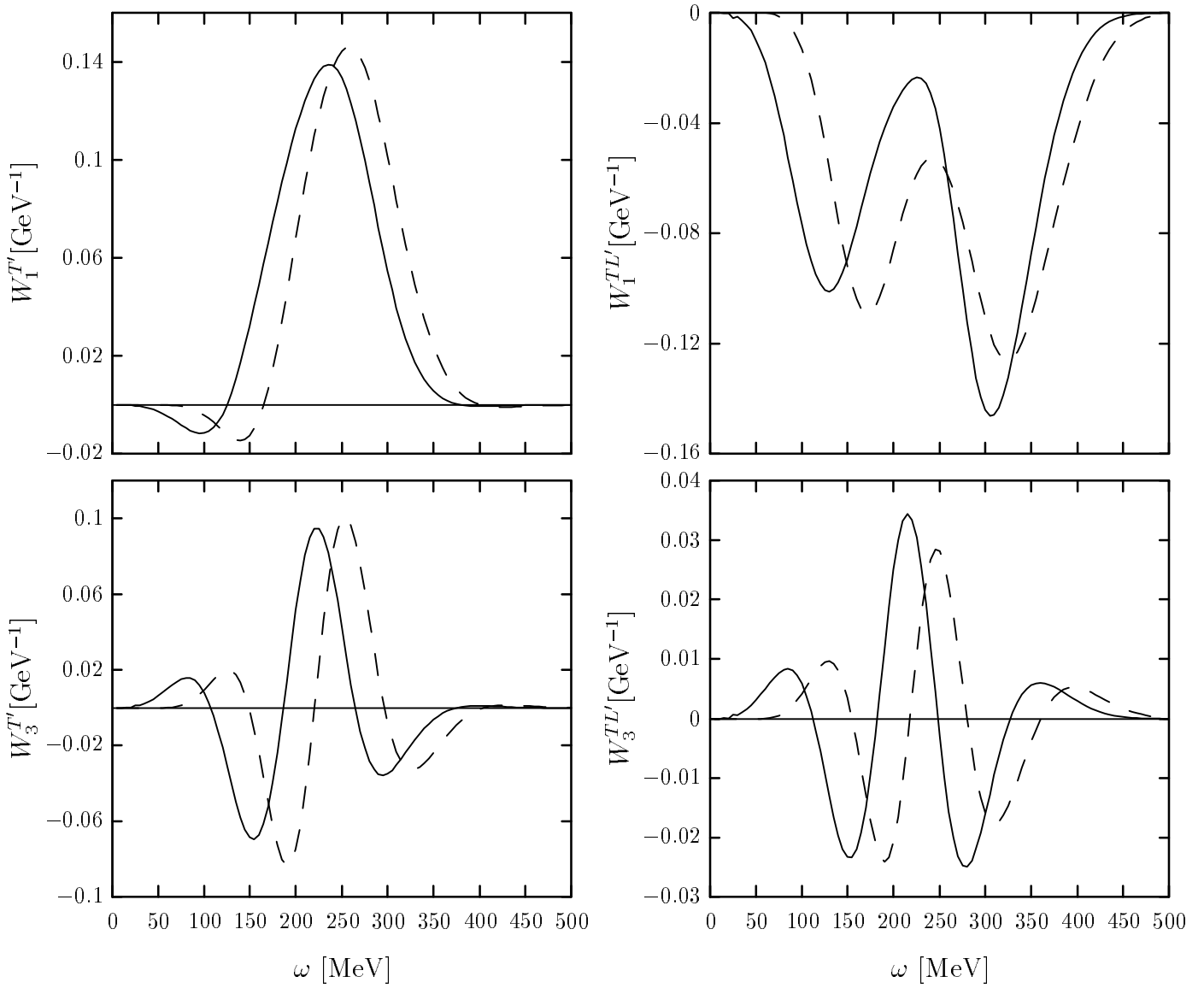


Figure 10

$^{39}\text{K}, q = 500 \text{ MeV}/c$

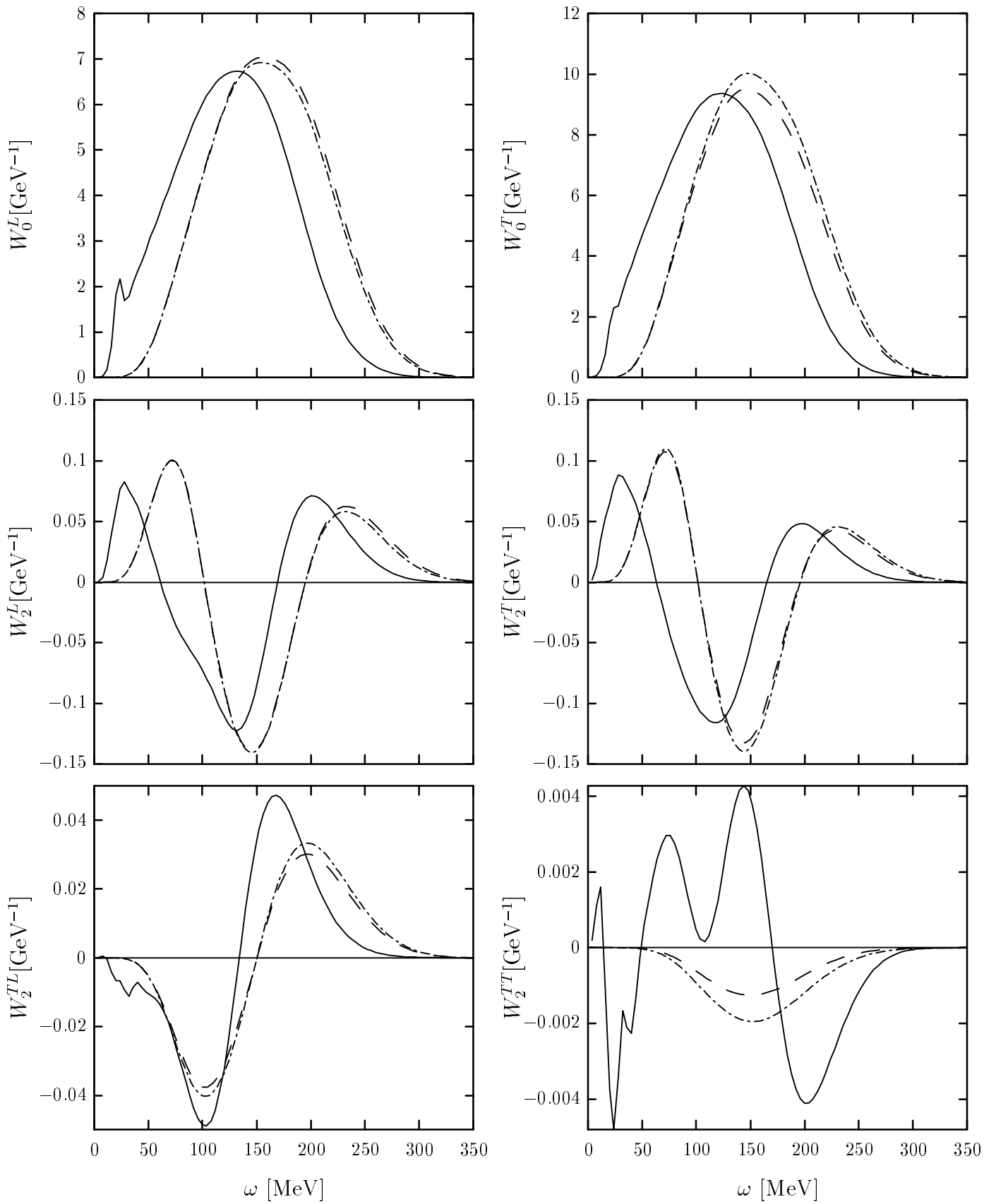


Figure 11

$^{39}\text{K}$ ,  $q = 500 \text{ MeV}/c$

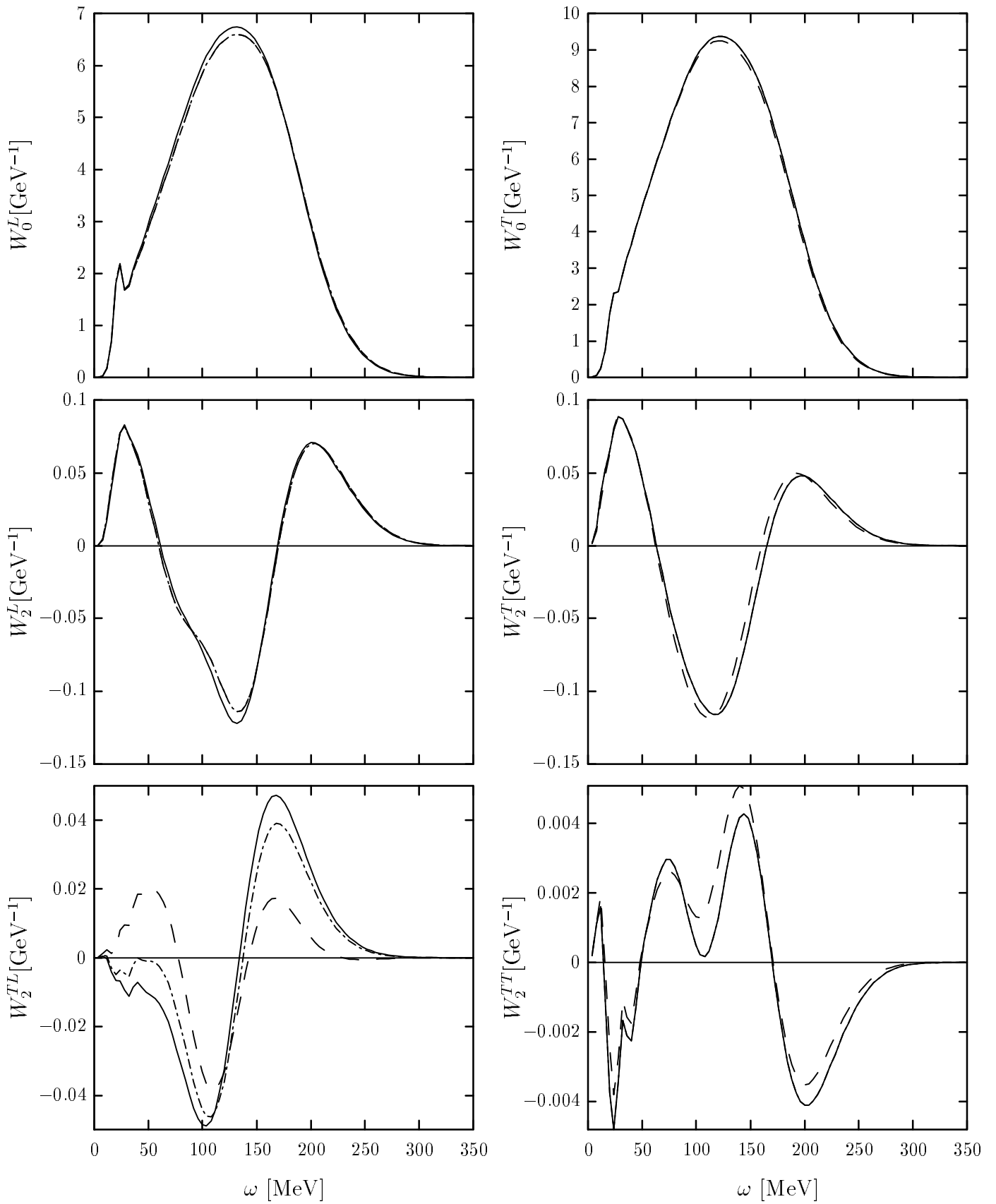


Figure 12

$^{39}\text{K}$ ,  $q = 500 \text{ MeV}/c$

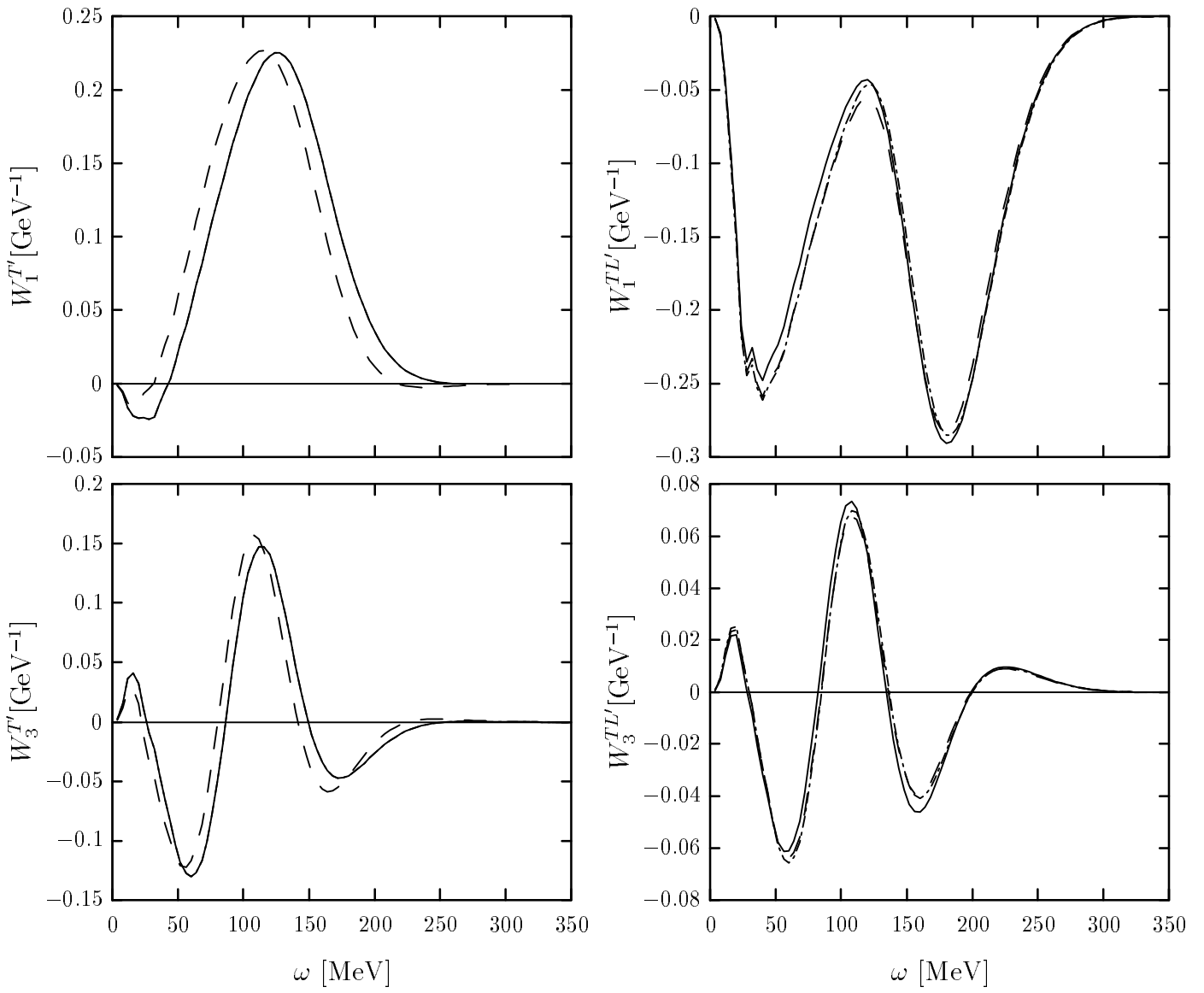


Figure 13

$^{39}\text{K}$

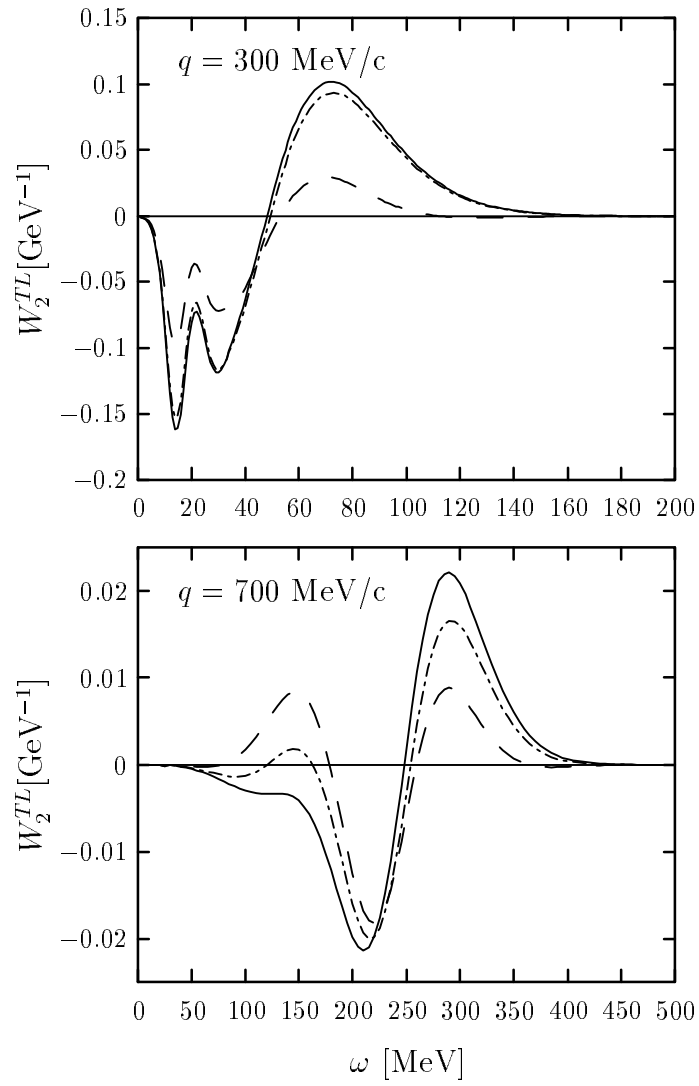


Figure 14